



EUROPEAN  
COMMISSION

Community Research



# CARBOWASTE

*Treatment and Disposal of Irradiated Graphite and Other Carbonaceous Waste*

**Grant Agreement Number: FP7-211333**



## Deliverable D-3.3.1

### First Radionuclide Inventory Data on Untreated Graphite / Evaluation for Direct Disposal

Author(s):

Dirk Vulpus, Werner von Lensa, Forschungszentrum Juelich GmbH  
Abbie Jones, University of Manchester; Christophe Guy, Jérôme Comte, CEA  
Alessandro Dodaro, ENEA; Grigorijus Duškesas, FI; Marius Iordache, INR

Document Number: CARBOWASTE-D-1001-3.3.1

Date of issue of this report: 24/03/2010

**Project co-funded by the European Commission under the Seventh Framework Programme (2007 to 2011) of the European Atomic Energy Community (EURATOM) for nuclear research and training activities**

#### Dissemination Level

<b>PU</b>	Public	
<b>RE</b>	Restricted to the partners of the CARBOWASTE project	
<b>CO</b>	Confidential, only for specific distribution list defined on this document	<b>X</b>

Start date of project: 01/04/2008

Duration: 48 Months



<b>CARBOWASTE</b>		
<b>Work package:</b> 3 <b>Task:</b> : 3.3	<b>CARBOWASTE document no:</b> CARBOWASTE-1001-D-3.3.1 (e.g. May 2008 as date of issue: 0805)	<b>Document type:</b> D=Deliverable
<b>Issued by:</b> Forschungszentrum Juelich GmbH (DE) <b>Internal no.:</b> CW1001-Deliverable-3-3-1-a		<b>Document status:</b> Review

<b>Document title</b>						
<b>First Radionuclide Inventory Data on Untreated Graphite / Evaluation for Direct Disposal</b>						
<b>Executive summary</b>						
<p>There are many types and sources of irradiated nuclear graphite waste and therefore it is unlikely a comprehensive database of empirical data for all this waste could ever be achieved. Therefore to gain an understanding of the location and stability of impurities / radioactive isotopes in selected irradiated graphite waste before and after various treatments. The latest scientific techniques will be employed to investigate where and how impurities / radioactive isotopes are located within virgin and irradiated nuclear graphite. Thus leading to a robust understanding of the value of various treatment options.</p> <p>This understanding may then be called upon in deciding and validating the most appropriate options for the disposal of irradiated nuclear graphite waste, so that it is also valid to evaluate the direct disposal of graphite without treatment. The results that come out from this task will also be added to the characteristics database in task 3.2 and 3.5.</p> <p>In this Task UoM, CIEMAT, FZJ work in characterisation after and before treatment. CEA, SCK-CEN, INR participate in the characterisation of their waste forms without treatment. WP6 has been involved to provide evaluation criteria for direct disposal.</p>						
<b>Revisions</b>						
Rev.	Date	Short description	Author	Review	Task Leader	WP Leader
00	dd/mm/yyyy	Issue	Name, Organisation	Name, Organisation <i>Signature</i>	Name, Organisation <i>Signature</i>	Name, Organisation <i>Signature</i>
01	24/03/2010	First issue	Vulpus FZJ <i>Vu</i>	Jones UoM	Vulpus FZJ <i>Vu</i>	Pina CIEMAT
02	dd/mm/yyyy	2 <sup>nd</sup> Issue				

## Table of Content

<b>1. OBJECTIVES OF THE TASK</b>	<b>6</b>
<b>2. INVESTIGATED SAMPLES</b>	<b>6</b>
2.1 Samples investigated at FZJ	6
2.1.1 Samples from Material Test Reactors (MTR)	6
2.1.2 Samples from High-Temperature Reactors (HTR)	8
2.2 Samples investigated at CEA	10
2.3 Samples investigated at CIEMAT	13
2.4 Samples investigated at ENEA	13
2.5 Samples investigated at FI / LEI	14
2.6 Samples investigated at INR	16
2.7 Samples investigated at SCK.CEN	18
2.8 Samples investigated at UoM	18
2.9 Samples investigated at ENS / IPNL ?	18
<b>3. DESCRIPTION OF CHARACTERISATION METHODS</b>	<b>18</b>
3.1 Characterisation Methods at FZJ	18
3.2 Characterisation Methods at CEA	20
3.3 Characterisation Methods at CIEMAT	22
3.4 Characterisation Methods at ENEA	22
3.5 Characterisation Methods at FI/LEI	24
3.6 Characterisation Methods at INR	25
3.7 Characterisation Methods at SCK.CEN	26
3.8 Characterisation Methods at UoM	27
3.9 Characterisation Methods at ENS / IPNL ?	29
<b>4. RADIONUCLIDE INVENTORIES</b>	<b>30</b>
4.1 Samples investigated at FZJ	30

4.1.1 Samples from Material Test Reactors (MTR)	30
4.1.2 Samples from High-Temperature Reactors (HTR)	31
<b>4.2 Samples investigated at CEA</b>	<b>33</b>
<b>4.3 Samples investigated at CIEMAT</b>	<b>37</b>
<b>4.4 Samples investigated at ENEA</b>	<b>37</b>
<b>4.5 Samples investigated at FI / LEI</b>	<b>38</b>
<b>4.6 Samples investigated at INR</b>	<b>39</b>
<b>4.7 Samples investigated at SCK.CEN</b>	<b>46</b>
<b>4.8 Samples investigated at UoM</b>	<b>47</b>
<b>4.9 Characterisation Methods at ENS / IPNL?</b>	<b>48</b>
<b>5. COMPILATION OF RESULTS</b>	<b>48</b>
<b>6. EVALUATION FOR DIRECT DISPOSAL</b>	<b>48</b>
<b>7. SUMMARY</b>	<b>48</b>
<b>8. REFERENCES</b>	<b>48</b>
<b>FORMAT OF INDIVIDUAL REPORTS</b>	<b>ERREUR ! SIGNET NON DEFINI.</b>

## **1. Objectives of the Task**

There are many types and sources of irradiated nuclear graphite waste and therefore it is unlikely a comprehensive database of empirical data for all this waste could ever be achieved. Therefore to gain an understanding of the location and stability of impurities / radioactive isotopes in selected irradiated graphite waste before and after various treatments. The latest scientific techniques will be employed to investigate where and how impurities / radioactive isotopes are located within virgin and irradiated nuclear graphite. Thus, extensive information will be supplied, which will lead to a more robust understanding of the value of various treatment and disposal options.

This understanding may then be called upon in deciding and validating the most appropriate options for the disposal of irradiated nuclear graphite waste, so that it is also valid to evaluate the direct disposal of graphite without treatment. The results that come out from this task will also be added to the characteristics database in task 3.2 and 3.5.

## **2. Investigated Samples**

### **2.1 Samples investigated at FZJ**

#### **2.1.1 Samples from Material Test Reactors (MTR)**

At the research centre of Jülich two types of material test reactors were in operation: the MERLIN reactor or FRJ-1, a light water moderated swimming pool reactor, and the DIDO reactor or FRJ-2, a heavy water moderated reactor. During the dismantling process of the MERLIN reactor and in preparation of the dismantling of the DIDO reactor graphite samples of the thermal column (see Figure 2.1.1) and of the graphite reflector (see Figure 2.1.2) have been taken. These samples were used for the following experiments.

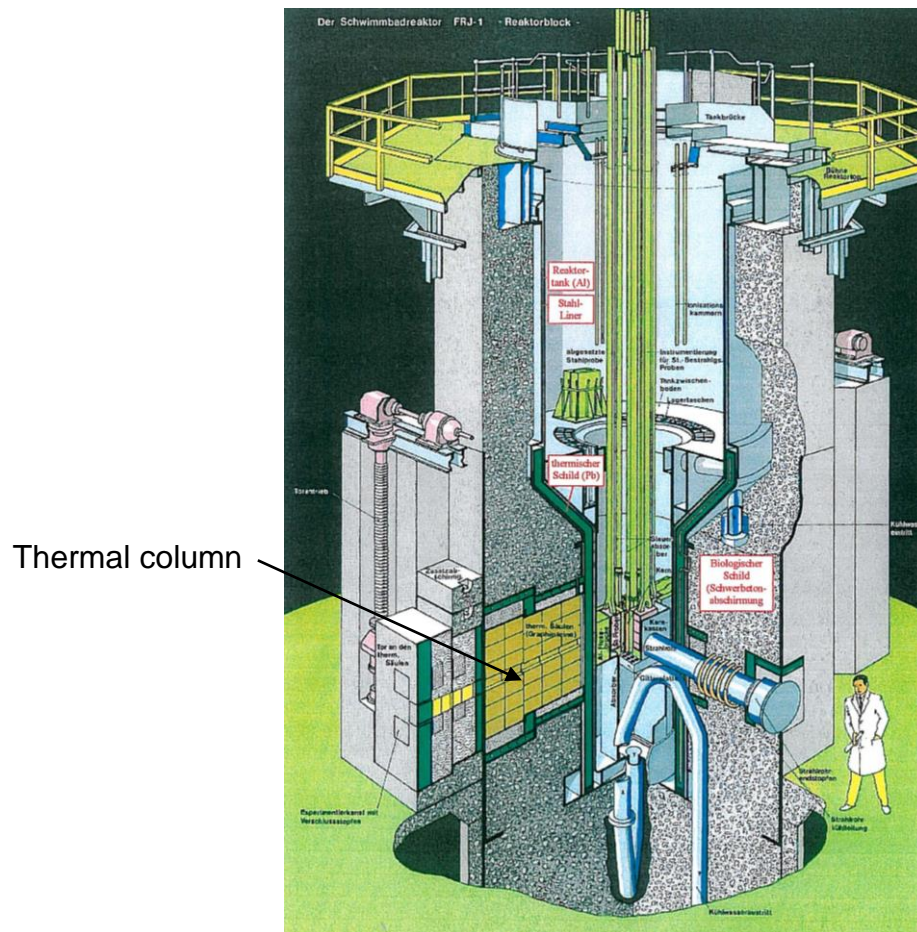


**Figure 2.1.1:** Schematic view of the MERLIN reactor (FRJ-1)



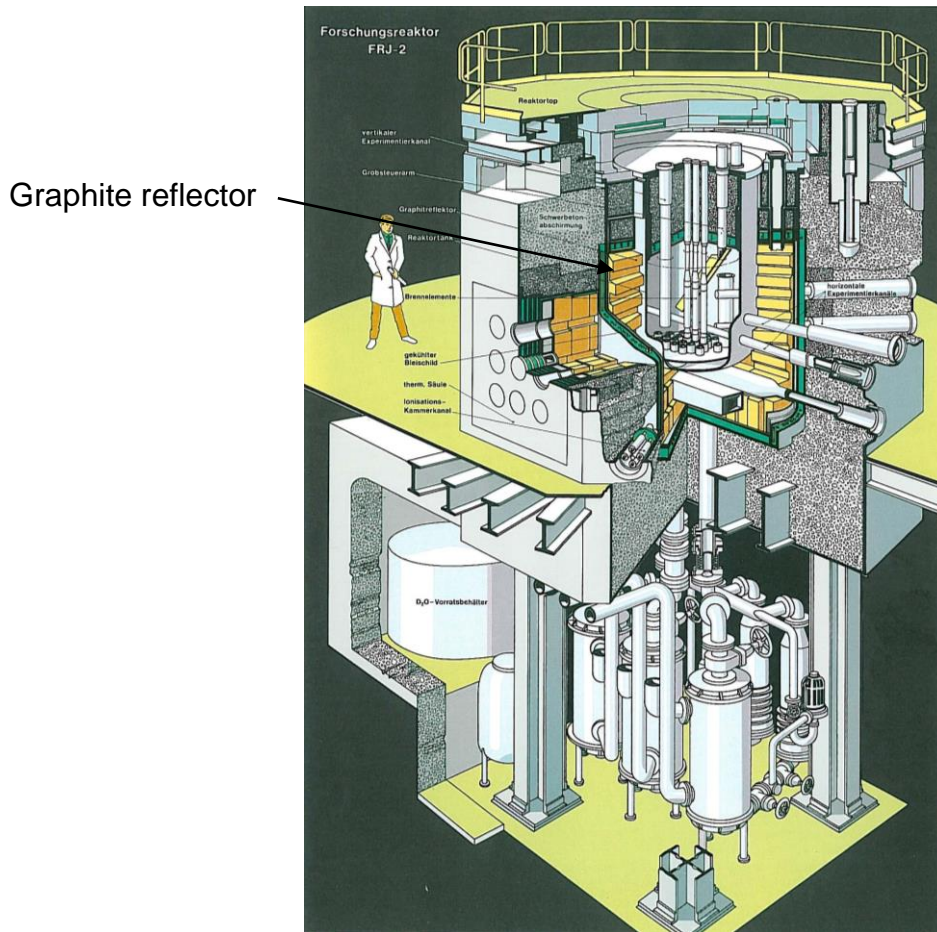


**Figure 2.1.2:** Schematic view of the DIDO reactor (FRJ-2)

### 2.1.2 Samples from High-Temperature Reactors (HTR)

At the research centre of Jülich a new type of high temperature reactors was developed. The operator was the Experimental Reactor Consortium (Arbeitsgemeinschaft Versuchsreaktor, AVR). The core of this reactor consisted of a pebble bed in which the fuel was embedded in graphite pebbles with a diameter of 60 mm. In these pebbles the fuel was dispersed as coated particles. The fuel zone of one pebble had a diameter of 50 mm and was enclosed by a 5 mm thick fuel-free graphite shell (see Figure 2.1.3). Flakings of this outer shell were used for the following experiments.



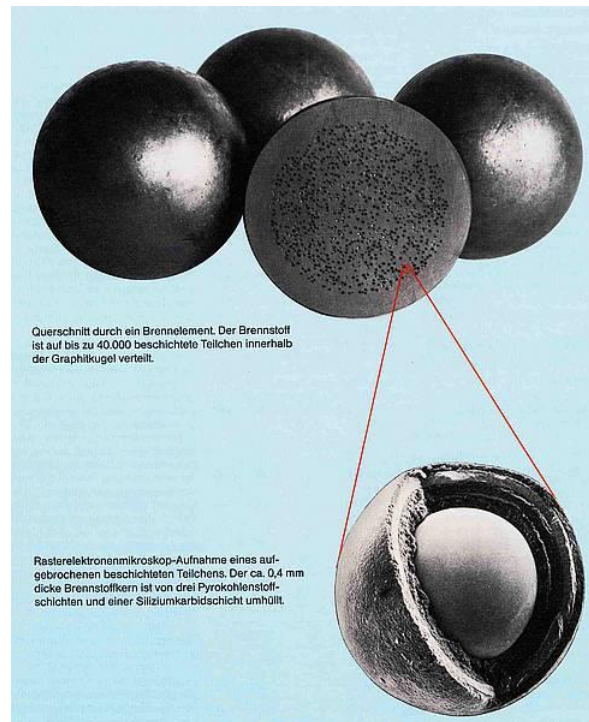


**Figure 2.1.3:** Sectional view of an AVR fuel pebble

The AVR reactor was a graphite-moderated gas-cooled high temperature reactor. Also the reflector was graphite (see Figure 2.1.4). In preparation of the dismantling of the reactor samples of the reflector have been taken. These samples were used for the following experiments.

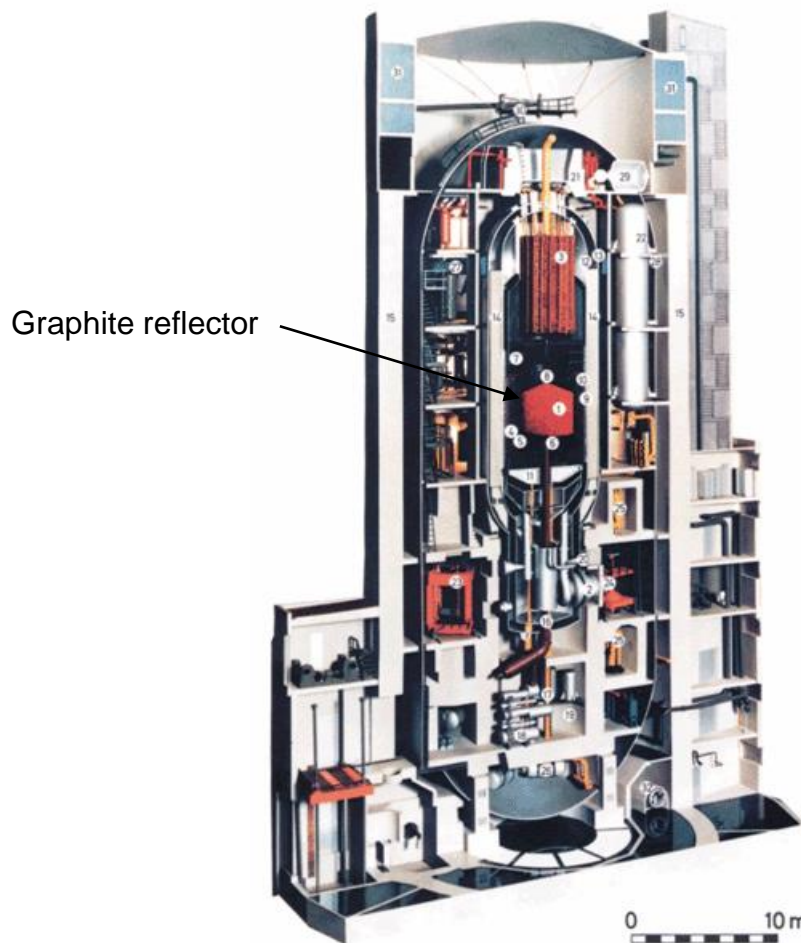


**Figure 2.1.4:** Schematic view of the AVR reactor

## 2.2 Samples investigated at CEA

### 2.2.1 Samples from the G2 UNGG (Uranium Natural Graphite Gas) reactor

Five core samples distributed over the lower half of the reactor were chosen to carry out studies on micro structural characterisation, behaviour of  $^{36}\text{Cl}$  during leaching, and to determine the activities of the radionuclides: four in the moderator (No. 27, 32, 36 and 42), and one in the reflector (No. 46). The five core samples are equidistant from each other, as shown in Figure 2.2.1.

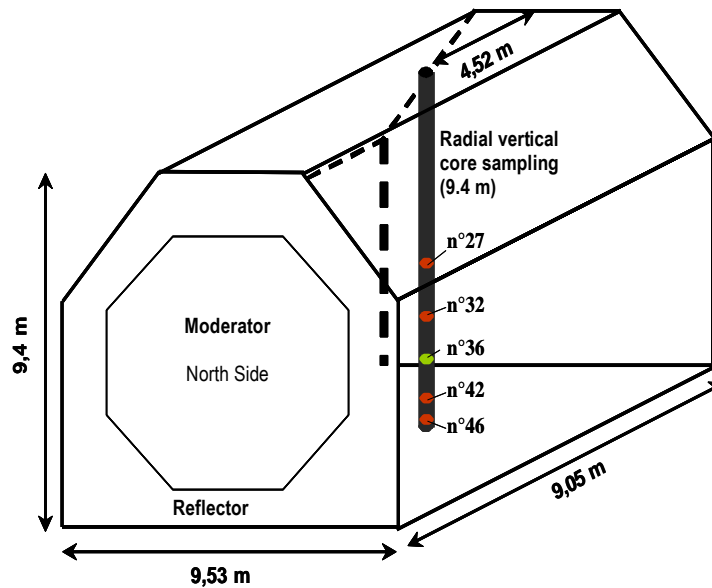


**Figure 2.2.1:** Representation of the G2 reactor with the vertical core sampling and the core samples selected

The dimensions of these core samples are around 130 mm long by a diameter of 63 mm, or around 650 g (Figure 2.2.2).

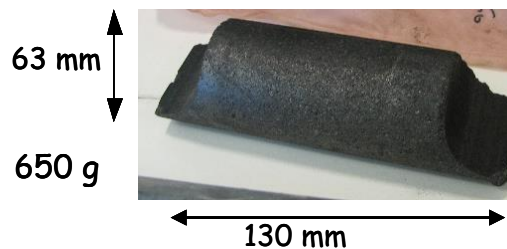


**Figure 2.2.2:** Dimension of G2 core samples

Table 2.2.1 contains the sampling levels and the functioning temperature of the reactor at the level of the core samples selected.

**Table 2.2.1:** Selected G2 samples (temperatures correspond to an estimated average for graphite)

Sample No.	Position	Assumed initial coke	Sampling level [m]	Temperature [°C]
G2-27	Moderator	Special A coke	13.60-13.80	327
G2-32	Moderator	Special A coke	14.60-14.80	320
G2-36	Moderator	Special A coke	15.40-15.60	314
G2-42	Moderator	Special A coke	16.60-16.80	309
G2-46	Reflector	Lockport Coke	17.40-17.60	284.7

For the purposes of the leaching tests, and in order to have several sampling tubes, the core samples were split into several samples. Table 2.2.2 shows the different samples analysed.

**Table 2.2.2:** G2 samples analysed

G2-27 G2-32 G2-42 G2-46	Powders arising from splitting operations representing an average core sample	3 samples taken from the ends and the middle of the core sample
G2-36		Removal of 11 samples along the core sample

#### 2.2.2 Samples from the St Laurent A2 UNGG reactor

10 core samples from St Laurent A2 were chosen to calculate the activity of the radionuclides. The following Table 2.2.3 shows the position of the samples in the reactor.

**Table 2.2.3:** Samples reference from St Laurent A2

Ref.	Channel	Height [mm]	Mass [g]
SLA2-103	F4M10C19	1.680	18.5446
SLA2-105	F4M10C19	2.460	21.6944
SLA2-110	F4M10C19	5.120	21.2202
SLA2-116	F4M10C19	7.880	21.5788
SLA2-119	F4M10C19	9.260	22.0051
SLA2-63	F5M7C17	1.680	23.761
SLA2-65	F5M7C17	2.460	18.7483
SLA2-71	F5M7C17	5.510	23.1647
SLA2-76	F5M7C17	7.880	23.6531
SLA2-79	F5M7C17	9.260	21.9857

The dimensions of these core samples are around 37 mm long by a diameter of 19 mm, or around 20 g (Figure 2.2.3).

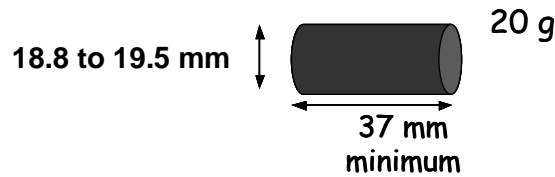


**Figure 2.2.3:** Dimension of G2 core samples

### 2.3 Samples investigated at CIEMAT

*/CIEMAT/ description and classification of sample material*

### 2.4 Samples investigated at ENEA

Due to the unavailability of the graphite from Romanian reactor, the samples of Irradiated Graphite used by ENEA for the Project, and below described, come from the Magnox Reactor of the Latina (Italy) Nuclear Power Plant.

The Nuclear graphite, specifically manufactured for use as a moderator or reflector within nuclear cores, consists of graphitic carbon of very high chemical purity to avoid absorption of low-energy neutrons and the production of undesirable radioactive species.

Besides the absence of neutron-absorbing impurities, reactor graphites are also characterized by a high degree of graphitization and no preferred bulk orientation. Such properties increase the dimensional stability of the graphite at high temperatures and in presence of high neutron flux.

The production of nuclear graphite consists in two steps: a carbonization or pyrolysis step and a graphitization step. During this graphitization process the graphite is purified with chlorine and hydrofluoric acid, and then pressed.

Nuclear graphite for the Magnox reactors were manufactured from petroleum coke mixed with coal-based binder pitch heated and extruded into bricks, and then baked at 1000 °C for several days. To reduce porosity and increase density the bricks are impregnated with coal tar at high temperature and pressure before a final bake at 2800 °C. Individual bricks were then machined into the final required shapes.

The Latina Reactor is Graphite moderated with fuel constituted by  $^{235}\text{U}$  and coated with Magnesium Oxide (MgO). The maximum burn-up was 5000 MWD/t. The operating period of the plant was 1963-1986, the starting nominal electrical power was 200 MW, but the value was reduced to 160 MW since 1969, with a cumulative output of about 26 TWh. The maximum operating temperature of the fuel was 450 °C. The

core consists of a 24-sided vertical prism made of graphite blocks in layers, assembled to form vertical cylindrical channels for fuel, control rods and neutron absorbers. The coolant was CO<sub>2</sub> in closed circuit. The graphite structure is divided into two parts: the central one (moderator or active core that hosts fuel and interstitial channels) and the lateral one (reflector). The floor bricks act both as reflector and moderator.

Several samples have been taken from different position in the core. For each sample a complete radiological characterization is scheduled by means of destructive and non-destructive measurements before and after the treatment. Unfortunately, due to a contamination event arisen in the laboratory during another experiment the area is actually not accessible, so that the data (dimensions, weight and inventory) for each sample are not available and the gamma measurements have been stopped till the complete radiological restoration of the area (foreseen for the middle of May).

For this reason only one sample's data are available and has been already characterized: it is the one labelled 04F04A1/I1, a prismatic one, taken from the inferior surface of a graphite brick, in the central channel (A1) at the bottom of the active core. The dimensions are 1.5 x 1.0 x 0.5 cm, and the weight is 1.8 grams.

## 2.5 Samples investigated at FI

The graphite samples from a fuel channel of the RBMK-1500 reactor of Ignalina NPP have been taken to represent top, central and bottom parts of a graphite sleeve. The graphite of the particular fuel channel of 10,700 MWd burn-up, which corresponds to 11.6 years of irradiation at the average power, has been selected for sampling.

Two irradiated samples Gr.13 and Gr.14 have been taken from the central part (at the active height of ~375 cm) of the graphite sleeve of the fuel channel and two other samples Gr.18 and Gr.16 from the top (at the active height of 28 cm) and the bottom (the plug fragment) of the fuel channel graphite (see Figure 2.5.1).

The biggest sample Gr.16 (146 g) taken from the bottom part of the fuel assembly is presented in Figure 2.5.2. The other samples weighted 2 g each. The original graphite sample Gr.16 had a shape of a cone. The samples for gamma spectrometric analysis have been scraped from the inner and outer surfaces of the graphite sample Gr.16.

To determine the level of homogeneity of activity distribution of gamma-emitters in the graphite the scraped samples from inner and outer surfaces of sample Gr.16 have been divided in three sub-samples from each surface.



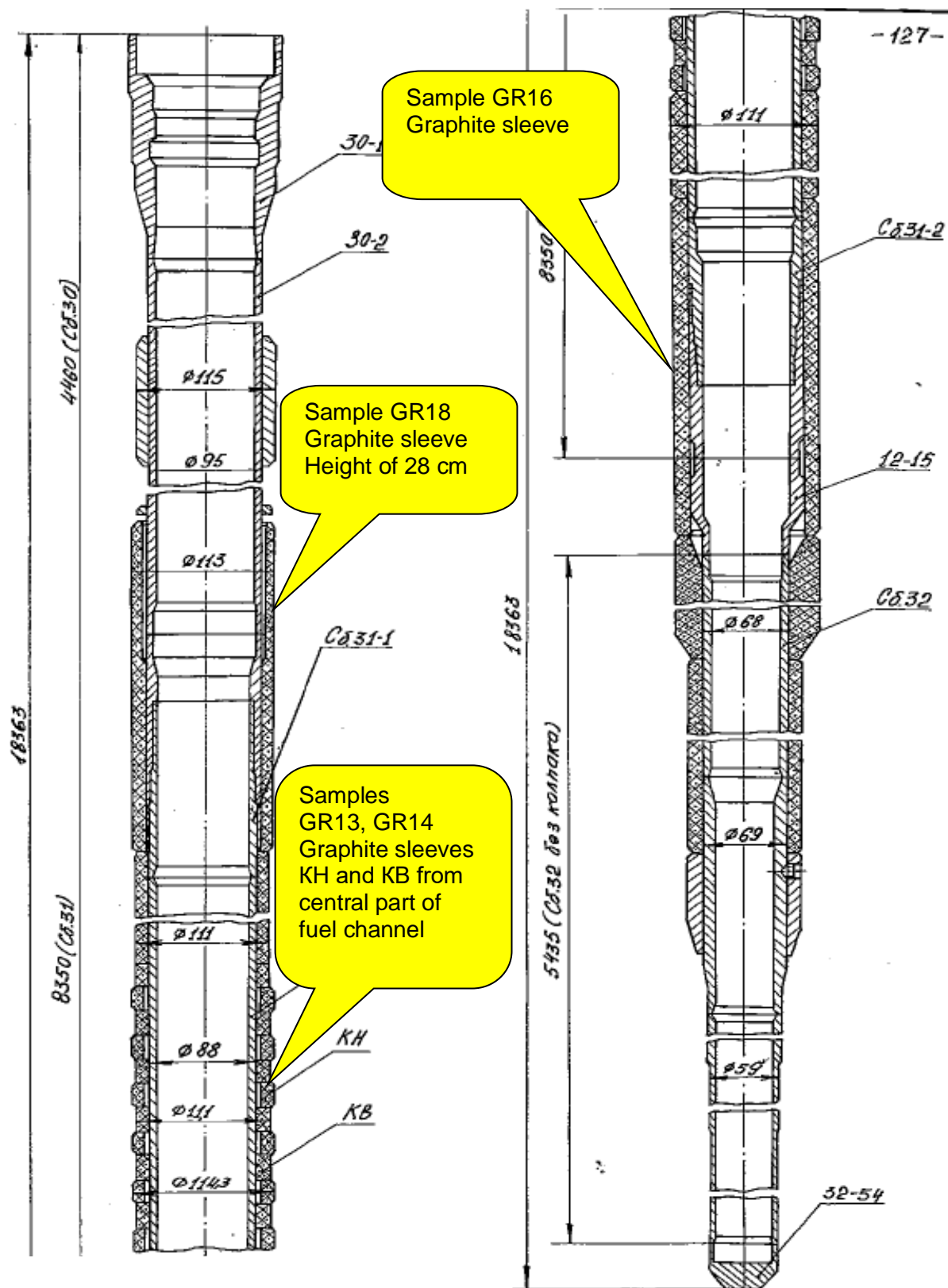


**Figure 2.5.1:** Top (on the left side) and bottom parts of the fuel channel

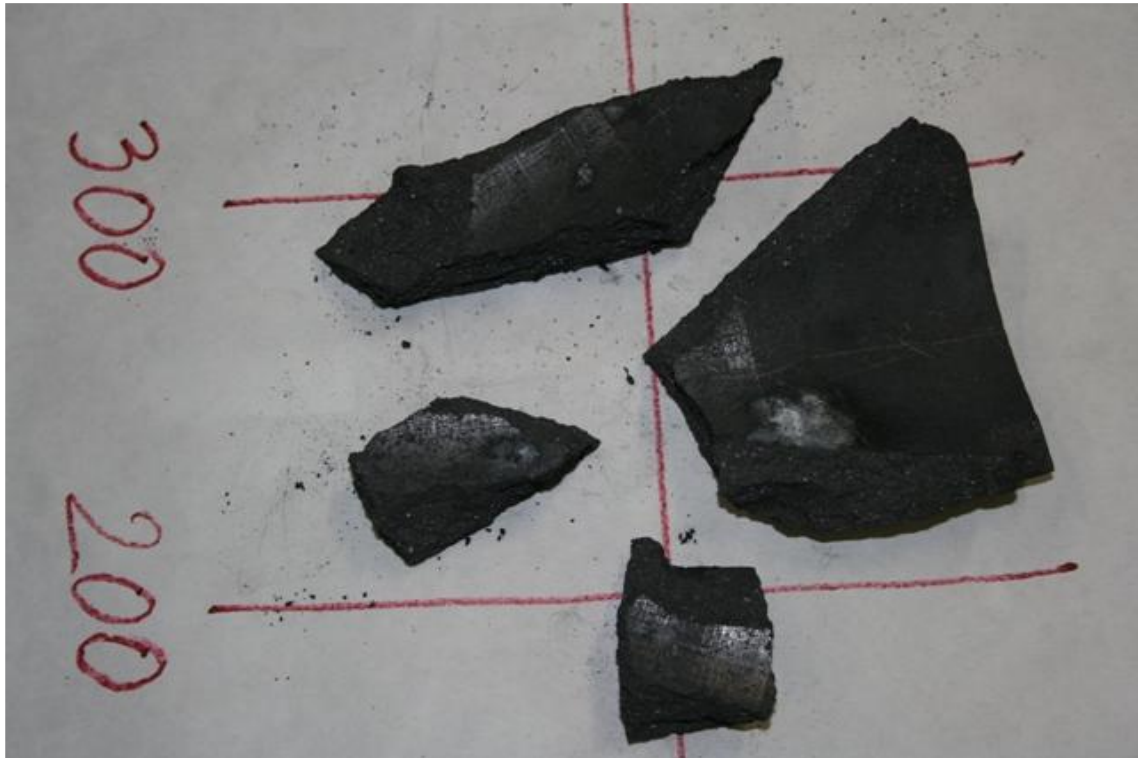


**Figure 2.5.2:** The biggest sample (Gr.16) of irradiated graphite taken from the bottom part of the fuel assembly

## 2.6 Samples investigated at INR

Samples of i-graphite investigated at INR arise from thermal column of material testing TRIGA reactor. The thermal column of TRIGA reactor is a graphite block with dimensions 1716 x 1144 x 710 mm; this is formed by 96 rectangular graphite cells (12 rows x 8 bricks) in aluminium cladding, with dimensions 144 x 144 x 770 mm, placed in the reactor pool. A number of graphite cells are already removed from the thermal column and stored.

In the first stage INR has investigated both sample of virgin and irradiated graphite. For the characterization of virgin graphite, polished samples have been mechanically prepared for elemental analysis and morphology investigations. In order to characterize the i-graphite, into a sealed niche the powder samples were mechanically prepared from different locations of a cell removed from thermal column.

Figure 2.6.1 shows a cross-section of the graphite cell used in TRIGA reactor. P1 – P8 represent the locations selected for i-graphite samples preparation in view of characterization.

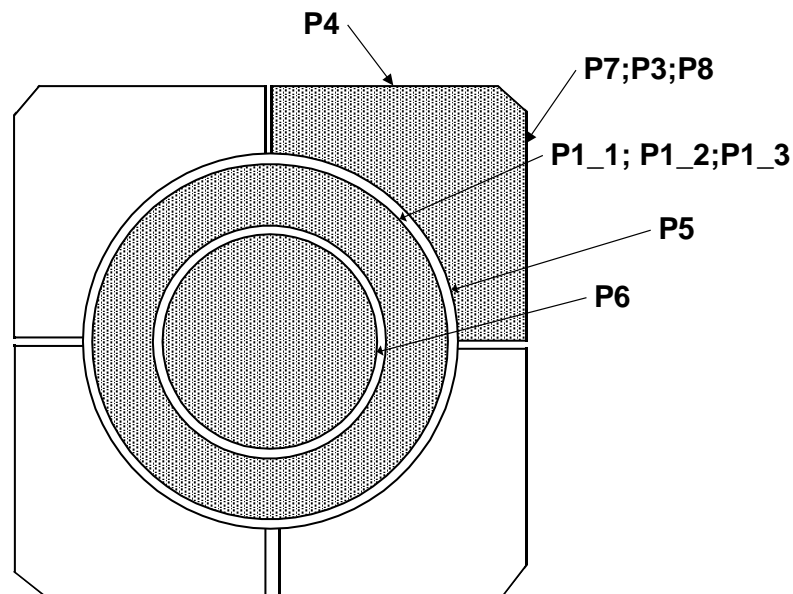


**Figure 2.6.1:** A cross-section of TRIGA reactor graphite cell

In this graph we see that a cell is constituted from a central cylindrical piece, followed by a pipe piece and finally four identically components, one for each cell corner. These four components have at outside a rectangular form and at the inside a concave form.

Also Figure 2.6.1 shows the pieces selected for preparation of irradiated samples. So, central cylindrical piece, pipe piece and one of the four pieces located in the cell corner were chosen. For the characterization of i-graphite from these three main components of the cell the following samples was prepared:

- One sample from central cylindrical piece (the sample codified P6);
- Three samples from external surface of pipe piece; the height of pipe was divided in three equal parts and from the upper part sample P1-1 was prepared, from the middle part sample P1-2 was prepared, and from the bottom part sample P1-3 was prepared;
- Five samples from the piece located in the cell corner as follow:
  - One from the middle part of cylindrical inside surface: sample P5;
  - Three from external surface of the piece: sample P7 from upper part, sample P3 from the middle part and sample P8 from the bottom part;
  - One from another external surface of piece: sample P4.

Powder form of these nine radioactive samples was chosen on account of its homogeneity. Characterization of i-graphite consists in gamma spectrometry using a special geometry and C-14 determination by total combustion of powder followed by counting using a liquid scintillation analyzer.

## 2.7 Samples investigated at SCK.CEN

SCK.CEN will characterise MTR graphite samples provided by INR. However, the regulatory body of Romania did not yet allow the distribution of these samples. Thus, INR was not yet been able to deliver the samples to SCK.CEN.

## 2.8 Samples investigated at UoM

The University of Manchester has acquired two irradiated graphite samples which were irradiated in materials test reactor (MTR) programmes (Raphael project) courtesy of NRG Petten. These graphites were irradiated as part of the Fp6 RAPHEAL framework and are from two graphite manufacturers: PCEA (GrafTech) is a fully graphitised nuclear grade graphite, extruded product which is from petroleum based coke, and NBG-10 (SGL) is fine grain extruded, semi-isotropic nuclear grade graphite manufactured from isotropic coke and pitch binder.

## 2.9 Samples investigated at ENS / IPNL ?

*/UoM/ description and characterization of sample material*

# **3. Description of Characterisation Methods**

## 3.1 Characterisation Methods at FZJ

The determination of the radionuclide inventory of the various graphite samples was carried out corresponding to the method described by Bisplinghoff et al. [3.1.1]. This method comprises the following steps:

- $\gamma$ -spectrometry of the (untreated) graphite sample for dominant  $\beta/\gamma$  emitters like Co-60, Cs-134/137, Ba-133, Eu-152/154/155;
- Incineration of the graphite sample in oxygen at 800 °C;
- Absorption of the flue gases in washing bottles with 0.1 M HNO<sub>3</sub> (for H-3 and Cl-36) and 4 M NaOH (for C-14);
- Liquid scintillation counting (LSC) of the scrubbing solutions;
- Acidic disintegration of the incineration residue;
- Measuring of Fe-55 with X-ray detector;
- Measuring of Sr-90/Y-90 by LSC;
- Possibly extraction of Ni-59/63.

The experimental procedure is illustrated in the following Figures: Figure 3.1.1 shows the incineration apparatus, Figure 3.1.2 a schematic view of the incineration apparatus and Figure 3.1.3 a scheme of the entire graphite characterisation method.



**Figure 3.1.1:** Apparatus for incineration of graphite samples

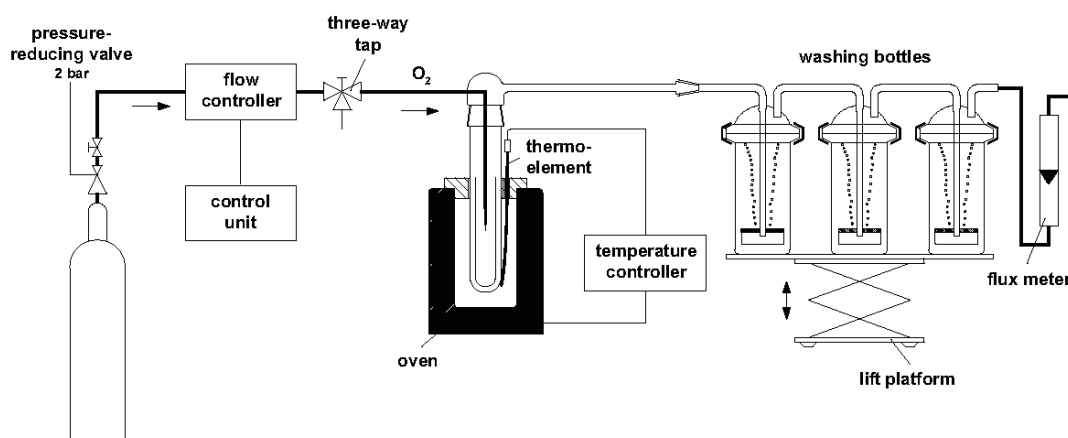


**Figure 3.1.2:** Schematic view of the incineration apparatus

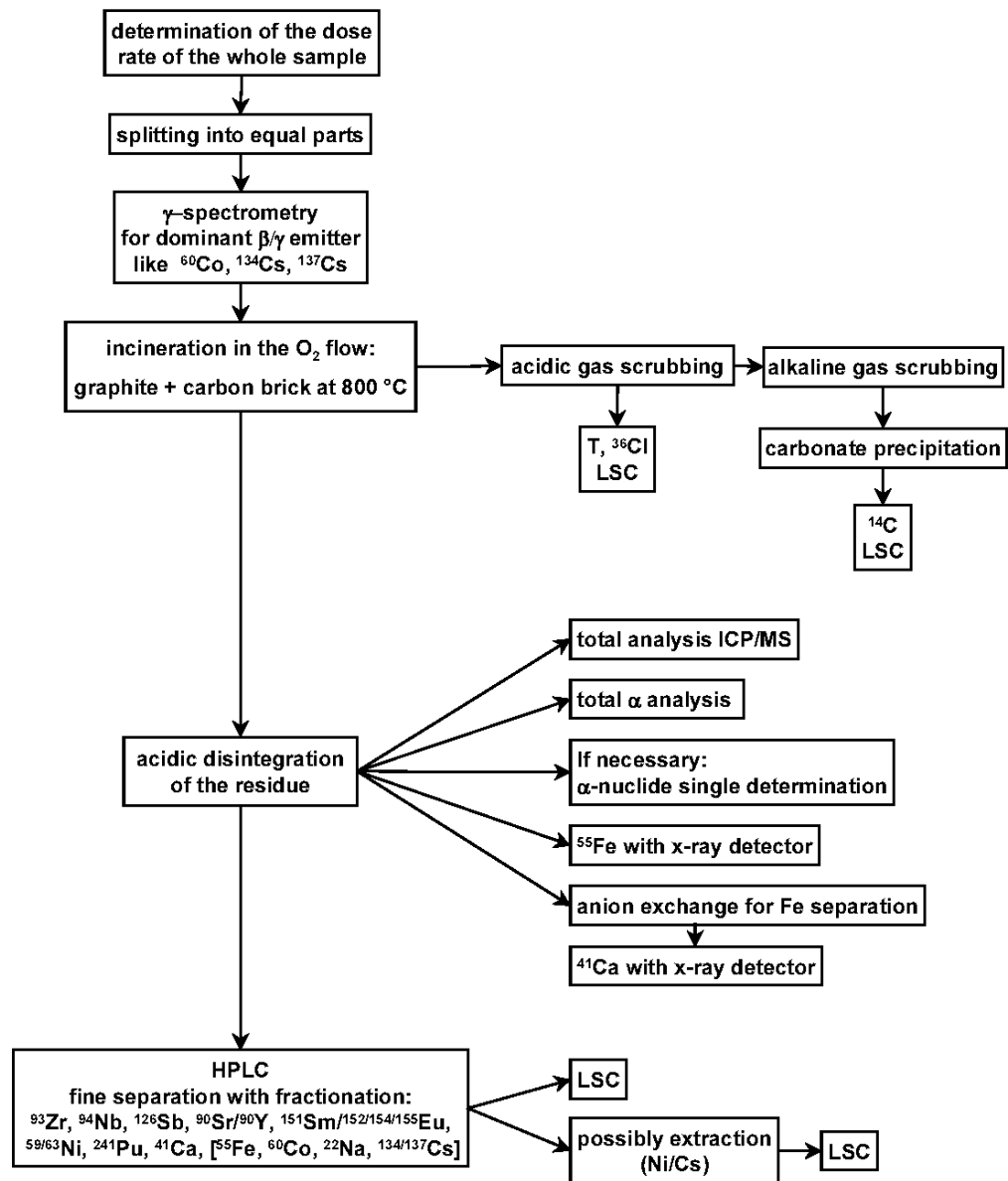


**Figure 3.1.3:** Scheme of graphite characterisation method

## 3.2 Characterisation Methods at CEA

### 3.2.1 Dissolution methods

All the reagents used have purity "for analyses".



### $^3\text{H}$ , $^{14}\text{C}$ , $^{63}\text{Ni}$

From the sample, two sub-samples of around 1 g were taken. Each sample was dissolved in hot acidic conditions with an open micro-wave reactor. Recovery of volatile nuclide (tritium and carbon) in a series of traps is associated with the dissolution device. Blank test without sample by using the same device and the same reagents was carried out before any dissolution in order to ensure the absence of any significant pollution.

### $^{36}\text{Cl}$

From the sample, two sub-samples of around 0.6 g were taken. Each sample taken was dissolved by mineralization in a Parr bomb.

## 3.2.2 Analyses methods

### Gamma activity measurement by gamma spectrometry

Gamma spectrometry was carried out on 50 ml of acidic solution (or around 0.25 g of graphite), in 50 ml standardised geometry in contact with a germanium hyperpur detector, for a measurement time of 54,000 seconds.

Direct gamma spectrometry was also carried out on the samples.

### $^3\text{H}$ activity measurement

On a neutralised aliquot from the solution, the tritium is separated through distillation before counting in liquid scintillation by an ultra low background analyser. The counting time is 3,600 seconds.

### $^{14}\text{C}$ activity measurement

On an aliquot of each of the basic traps, oxidation of the carbon in  $\text{CO}_2$  form was achieved. The  $\text{CO}_2$  thus formed is trapped in a specific counting liquid for  $^{14}\text{C}$  with measurement by liquid scintillation through an ultra low background analyser. The counting time is 3,600 seconds. The activities of each bubbler are added and applied to the sample. The activity of the No. 3 bubbler should be negligible with regard to the No. 1 bubbler, which guarantees a chemical yield of 100%.

### $^{63}\text{Ni}$ activity measurement:

On an aliquot of the solution, after adding a Ni tracer, selective separation of the Ni is obtained by liquid-liquid extractions. The  $^{63}\text{Ni}$  is measured by liquid scintillation through an ultra low background analyser. The counting time is 3600 seconds. The chemical yield is approximately 85%.

### $^{36}\text{Cl}$ activity measurement

The chlorine is separated from the solution by precipitation and purification of the solution taken from this precipitate on anions exchange resin. An aliquot of the eluate is measured by liquid scintillation through an ultra low background analyser. The

counting time is 3,600 seconds. The chemical yield, measured by ionic chromatography, is approximately 95%.

### 3.3 Characterisation Methods at CIEMAT

### 3.4 Characterisation Methods at ENEA

#### 3.4.1 Gamma Spectrometry

The gamma emitters contained in the sample are characterized by means of a gamma spectrometry system equipped with LABSOCS software. The measurement configuration and the samples' chemical and physical characteristics have been reproduced with the maximum accuracy available. To minimize the Minimum Detectable Activity, the sample has been inserted in an ultra-low background lead housing.



**Figure 3.4.1:** HPGe detector equipped with LABSOCS (Laboratory Sourceless Calibration Software)

### 3.4.2 Liquid Scintillation Counting

The analysis of Tritium,  $^{14}\text{C}$  and  $^{36}\text{Cl}$  is made by a technique that involves a controlled combustion of a sample of grinded Graphite in Tube Furnace under Oxygen flow, to convert all the  $^{14}\text{C}$  into Carbon Dioxide ( $\text{CO}_2$ ),  $^3\text{H}$  in water vapour, either generally trapped by gas bubbler filled with trapping agents.



**Figure 3.4.2:** Furnace equipped with Drechsel bottles to trap carbon from graphite combustion

A silica glass work-tube inside a specially built two-zone furnace, independently heat-controlled: 1<sup>st</sup> zone, sample in a silica glass combustion boat; 2<sup>nd</sup> zone, copper-oxide catalyst.

The  $^{14}\text{C}$  is extracted by bubbling the carbon dioxide  $\text{CO}_2$  gas through an alkaline liquid trapping agent such as aqueous sodium hydroxide or ethanolamine or employing solid trapping agents such as molecular sieves or solid adsorbents (such as Carbosorb, Calcium hydroxide).

For  $^{36}\text{Cl}$  contents in graphite samples, an Analytical Method similar to the  $^{14}\text{C}$  measurement method will be assessed, using a different and appropriated trapping agent at the exit of the Tube Furnace such as Nitric Acid  $\text{HNO}_3$  0.1 M.

The Tritium is converted in water vapour, the trapping agent is also  $\text{HNO}_3$  0.1 M. That means that the analysis should be performed on different samples.

In order to ensure complete conversion of all thermal decomposition products given by the sample combustion, these last are swept over a catalyst such as Copper Oxide heated to a temperature of 750 °C.

The content of radionuclides in all trapping media is determined by Liquid Scintillation Counting. Samples are dissolved or suspended in a cocktail containing an aromatic solvent and small amounts of other additives known as fluors or scintillators. Beta particles emitted from the sample transfer energy to the solvent molecules, which in turn transfer their energy to the fluors; the excited fluor molecules dissipate the energy by emitting light. In this way, beta emission results in a pulse of light. Scintillation cocktails often contain additives that shift the wavelength of the emitted light to make it more easily detected.

Regarding the  $^{63}\text{Ni}$  characterization, a weighed sample of graphite is placed in a round-bottom flask and 20 mL of concentrated acids mixture ( $\text{H}_2\text{SO}_4:\text{HNO}_3:\text{HClO}_4 = 4:1:1$ ) are added. The mixture is heated to 150–200 °C with reflux until a clear solution is obtained (1.5–2 h). The solution is then evaporated to 1–2 mL. The sample so prepared is mixed with Ultima Gold LLT scintillation cocktail in a 20 mL polyethylene vial and measured by a Liquid Scintillation Counter (LSC) using a low energy beta nuclides window.

The above mentioned preparation of the samples for Liquid Scintillation Counting is preceded by the grinding of the graphite with an impact analysis mill IKA A-11 Basic, able to reduce soft, medium-hard and brittle materials with a Mohs' hardness up to 6–7 (Graphite: 1–1.5 Mohs). Graphite samples are initially broken down into small pieces (by hammer).

### 3.5 Characterisation Methods at FI

Graphite samples from the RBMK-1500 reactor of the Ignalina NPP have been analysed by methods of the non-destructive and destructive analysis. The gamma-ray spectrometer with two calibrated HPGe detectors was used for the non-destructive analysis.

For the destruction and dissolving of graphite, concentrated acids  $\text{H}_2\text{SO}_4$ ,  $\text{HNO}_3$  and  $\text{HClO}_4$  (ratio 4:1:1, respectively) have been used. It should be noted that not all the material was completely dissolved by this method. After filtering, the residue has been dried, its mass has been determined, and the fraction of dissolved graphite has been estimated.

The wet acidifying procedure with two catches ensured 94% chemical recovery of radiocarbon. Concentrations of radionuclides C-14 and Cl-36 in prepared graphite samples have been measured with the liquid scintillation counter Quantulus-1220 (Wallac).

The activity of radionuclide C-14 in the graphite samples of the RBMK-1500 reactor core after 11.6 years of irradiation has been also calculated by MCNPX code coupled with CINDER code.

### 3.6 Characterisation Methods at INR

Regarding the characterization of i-graphite, INR contribution was concentrated on the development and application of characterization methods for powder samples prepared on a 2 mm depth of graphite cell. The characterization methods of i-graphite used at INR consisted in identification and determination of  $\beta/\gamma$  emitting radionuclides by gamma-ray spectrometry and determination of C-14 content by liquid scintillation counting.

Determination of activity concentration of beta-gamma emitting radionuclides has been performed by high resolution gamma spectrometry analysis using a portable ORTEC detector equipped with a digiDART powerful multichannel analyzer. The main features of the spectrometric chain are:

- HPGe coaxial detector type “pop-top”, model no. GEM-15P4 CFG-PMOD4-7;
- Portable spectrometric system with autonomous supply, type ORTEC digiDART with 16384 channels;
- GAMMAVISION software for acquisition and analysis of spectral data.

The i-graphite powder samples have been mechanically prepared into a sealed niche. This form of sample was chosen because of its homogeneity. In the first stage was chosen a geometry in which the powder samples of 5 g weight was placed in plastic boxes. Samples from the same i-graphite brick, but from different locations have been prepared. The measurement geometry chosen is the following:

- The HPGe coaxial detector is in vertical position;
- The plastic box with i-graphite powder is placed right to the detector.

Both of them were located into a lead shielded chamber, so that the distance detector-sample is zero.

Presently, we are studying a measurement geometry in which powder samples of 0.3 g weight are placed in 20 ml glass vials. The measurement geometry was slightly modified in order to reduce the i-graphite powder quantity necessary for characterization.

For the energy and efficiency calibration of the spectrometric chain, a reference graphite source with the same form as i-graphite powder was prepared as follows: 5 g of virgin graphite (the same type with those in thermal column of TRIGA reactor) were mixed with 5 ml of standard Amersham solution contaminated with Am-241, Ba-133, Cs-137 and Co-60, then dried and homogenized. The total activity of the reference sample used for energy and efficiency calibration is presented in the following Table 3.6.1.



**Table 3.6.1:** Total activity of the energy reference sample

Radionuclide	Activity (Bq)
Am-241	507.65 ± 3.5%
Ba-133	23.80 ± 3.0%
Cs-137	110.45 ± 3.2%
Co-60	58.78 ± 3.2%

In the case of geometry measurement in which powder samples of 0.3 g weight in 20 ml glass vial were used, the reference source was prepared as follows: 0.3 g of virgin graphite were mixed with 0.4 ml of standard Amersham solution contaminated with Am-241, Ba-133, Cs-137 and Co-60, then dried and homogenized. The total activity of radionuclides for reference source is presented in the following Table 3.6.2.

**Table 3.6.2:** Total activity of the geometry reference sample

Radionuclide	Activity (Bq)
Am-241	913.14 ± 3.6%
Ba-133	143.97 ± 3.8%
Cs-137	791.71 ± 3.4%
Co-60	327.38 ± 3.1%

For a part of powder samples prepared as described above, INR has designed and tested the method for determination of C-14 content in i-graphite. The process consists of two steps:

1. Graphite combustion using the PerkinElmer Sample Oxidizer Model 307. During the combustion process,  $^{14}\text{C}$  is oxidized to gaseous carbon dioxide. An absorbent, Carbo-Sorb E, traps the radioactive carbon dioxide and forms a carbamate to be flushed into the  $^{14}\text{C}$  counting vial using the  $^{14}\text{C}$  scintillator, Permafluor E+, as a rinsing media. The reagent metering pumps were set to deliver 10 mL Permafluor E+ and 10 mL Carbo-Sorb E. The combustion timer was set for 1.17 minutes.
2. Counting of the vials in a Packard Tri-Carb 2100 liquid scintillation analyzer using recommended  $^{14}\text{C}$  counting conditions. The samples and blank vials were counted for 40 minutes.

### 3.7 Characterisation Methods at SCK.CEN

For the analysis of volatile nuclides ( $^3\text{H}$ ,  $^{14}\text{C}$ ,  $^{36}\text{Cl}$ ), combustion of the samples will be performed. These nuclides, which are beta-emitters, will be measured by liquid scintillation counting. Non-volatile nuclides will be analysed after acid dissolution of the graphite.



### 3.8 Characterisation Methods at UoM

#### 3.8.1. X-ray Tomography

Computerised x-ray tomography is a non destructive technique that allows the 3D microstructure of irradiated graphite to be analysed. This technique involves sending an X-ray beam through the material and recording the transmitted beam using a charged coupled device camera as shown in Figure 3.8.1. The ratio of transmitted to incident photons is related to the integral of the absorption coefficient of the material along the path that the photons made through the material. Using an empirical law, the absorption coefficient can be related to the density, the atomic number and in certain cases, the energy. The resulting image is a projection of a volume in a given 2D plane. The method of acquiring a 3D image is to obtain radiographs whilst rotating the sample between  $0^\circ$  and  $180^\circ$ . An algorithm (filtered back-projection) is applied to reconstruct the volume from the 2D radiographs.

This CT data was used to determine porosity and density of the BEPO graphite. The smallest porosity or characteristics that can be identified however are limited to the resolution of the 2D radiographs which is determined by the sample size and CCD camera used.

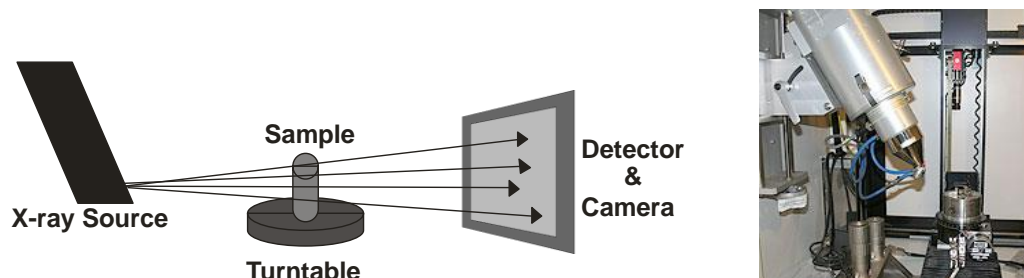


**Figure 3.8.1:** A) Schematic and B) photograph of X-ray tomography scanner

Tomography images were collected using the X-TEK HMX CT instrument using the parameters outlined in Table 3.8.1. In addition, a rotation of  $0.3^\circ$  with 32 frames and a camera exposure time of 160 s were also applied. A voxel size of  $21.4 \mu\text{m}$  was resolved.

Irradiated graphite analysis was performed with the samples contained within a 'harwell can', this ensured that no radioactive graphite dust would contaminate the tomography equipment. No filter was applied during the analysis as the can is made out of aluminium thus acting as a filter. A calibration of the can's thickness versus attenuation using highly orientated pyrolytic graphite (HOPG) as a reference standard inside the can is shown in Figure 3.8.2 where intensity shown to exhibit a linear relationship with thickness.

**Table 3.8.1:** Tomography experimental parameters

Parameters	Settings
Target	Copper
Filter	None
Detector	Beryllium
Voltage	95 kV
Current	105 $\mu$ A

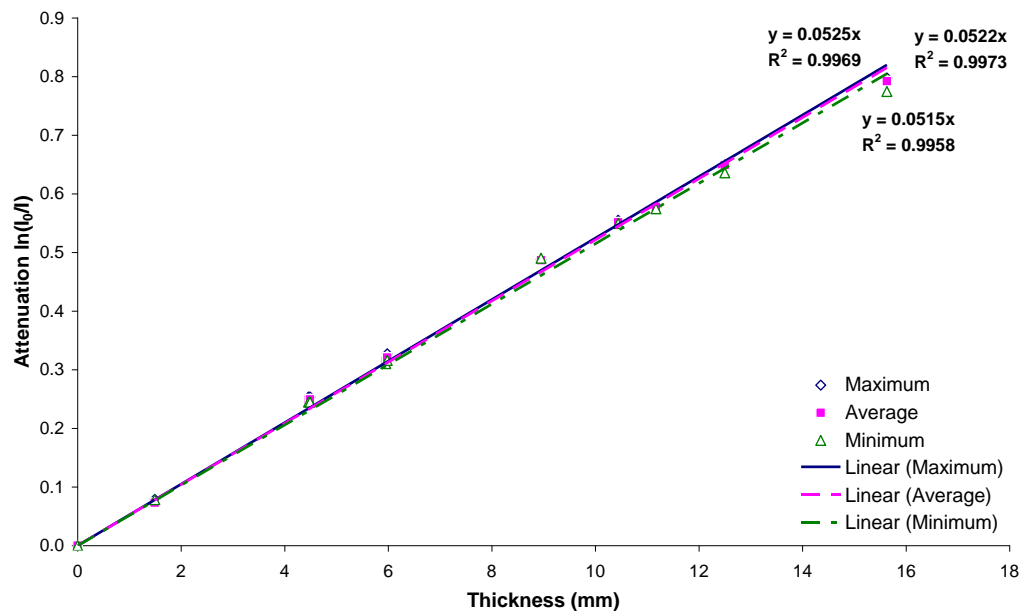


**Figure 3.8.2:** Calibration graph of thickness of HOPG sample inside a harwell can versus the attenuation intensity of the transmitted incident photons that have passed thorough the HOPG sample

### 3.8.2. Autoradiography

Autoradiography provides a visual distribution pattern of radiation present in the surface of a sample, depending on isotope energy. Autoradiography can therefore determine  $\beta$  and  $\gamma$  radiation present within nuclear graphite with energy above 0.018 MeV. Weak  $\beta$ -emitting isotopes and  $\alpha$  isotopes are stopped by the coating on the phosphorous storage film (recording medium). Autoradiography is a qualitative technique used to analyse high energy  $\beta$  and  $\gamma$  isotopes present within a nuclear graphite sample.

The phosphor storage screens comprise of fine crystals of  $\text{BaFBr:Eu}^{2+}$  in an organic binder. Upon exposure to radiation the  $\text{Eu}^{+2}$  is excited to the oxidised  $\text{Eu}^{3+}$  state and the  $\text{BaFBr}$  is reduced to  $\text{BaFBr}^-$ . The phosphor storage screen releases this energy when exposed to light of an appropriate wavelength. Excited electrons fall to the ground state thus releasing energy in the form of blue light. The emitted light passes through a photomultiplier detector which converted to produce an electric current proportional to the activity in the sample.

The advantages of this technique include reduced exposure time compared to traditional autoradiography using X-ray film and increased sensitivity with a linear dynamic range of 1 to 100,000 which allows both weak and strong energy isotopes to be analysed simultaneously

A Typhoon 9410 Amersham instrument has been used throughout this study. Sample size, or preferentially diameter is shown to have significant effect on the autoradiography results. Autoradiography analysis of graphite samples thicker than 1 cm have proved difficult to analyse with the high energy radionuclide's saturating the film after only a 4–6 hours, making comparison between graphite samples that have acquired varying levels of dose or exposure inconclusive.

In total 60 samples were analysed. The sample size was 1 mm in diameter and manually cut from using a saw. The autoradiography screen was wiped clean after each use using a light box and a lint free cloth. The samples were placed on the screen in a glove box and left for 20 hours. This length of time was determined as sufficient exposure time without saturating the film due to the activity present in the graphite and will vary for each type of sample being analysed.

Analysis of the film performed using the Amersham (wavelength of 633 nm) and a pixel size of 50 microns. The average intensity, standard deviation, variance, minimum and maximum intensity and area are calculated. This allows the background to be deducted from analysis and documents any errors between results.

### 3.9 Characterisation Methods at ENS / IPNL ?

## 4. Radionuclide Inventories

### 4.1 Samples investigated at FZJ

#### 4.1.1 Samples from Material Test Reactors (MTR)

Table 4.1.1 summarises the radionuclide inventory of a typical sample from the thermal column of the MERLIN reactor (FRJ-1) and Table 4.1.2 summarises the radionuclide inventory of a typical sample from the reflector of the DIDO reactor (FRJ-2). The inventory of activation products like H-3, C-14, Fe-55, Co-60 and Eu-154/155 is much higher in DIDO graphite than in MERLIN graphite. This is reasonably on account of the different graphite types: the reflector graphite of the DIDO reactor is significantly closer at the reactor core than the graphite of the thermal column of the MERLIN reactor and, therefore, the neutron flux is much higher.

**Table 4.1.1:** Radionuclide inventory of a typical sample from the thermal column of the MERLIN reactor (FRJ-1)

Nuclide	Activity [Bq/g]
H-3	3.2E+03 ( $\pm 10\%$ )
C-14	3.8E+02 ( $\pm 10\%$ )
Fe-55	7.5E+01 ( $\pm 10\%$ )
Co-60	3.4E+00 ( $\pm 20\%$ )
Sr-90	n. d.
Cs-134	n. d.
Cs-137	n. d.
Ba-133	1.0E+01 ( $\pm 9\%$ )
Eu-152	4.6E+02 ( $\pm 13\%$ )
Eu-154	1.2E+01 ( $\pm 9\%$ )
Eu-155	n. d.

\* Date of reference: 01/02/2010

**Table 4.1.2:** Radionuclide inventory of a typical sample from the reflector of the DIDO reactor (FRJ-2)

Nuclide	Activity [Bq/g]
H-3	2.6E+06 ( $\pm 10\%$ )
C-14	9.8E+04 ( $\pm 10\%$ )
Cl-36	n. d.
Fe-55	9.7E+03 ( $\pm 10\%$ )
Co-60	8.9E+03 ( $\pm 14\%$ )
Ni-59/63	n. d.
Sr-90	n. d.
Cs-134	4.3E+02 ( $\pm 16\%$ )
Cs-137	7.7E+01 ( $\pm 18\%$ )
Ba-133	2.0E+02 ( $\pm 12\%$ )
Eu-152	n. d.
Eu-154	2.6E+03 ( $\pm 4\%$ )
Eu-155	1.6E+03 ( $\pm 9\%$ )

\* Date of reference: 01/02/2010

#### 4.1.2 Samples from High-Temperature Reactors (HTR)

Table 4.1.3 summarises the radionuclide inventory of a typical sample from the outer shell of a fuel pebble from the AVR reactor and Table 4.1.4 summarises the radionuclide inventory of a typical sample from the reflector of the AVR reactor. As expected, the inventory of all radionuclides is higher in the reflector graphite than in the fuel pebble graphite. This is on account of the longer neutron irradiation time of the reflector graphite (the entire operation time of the reactor).

The relatively high amount of fission products like Sr-90 and Cs-137 at both graphite types is conspicuous. This high contamination comes from the initial operation time of the AVR reactor.

**Table 4.1.3:** Radionuclide inventory of a typical sample from the outer shell of a fuel pebble from the AVR reactor

Nuclide	Activity [Bq/g]
H-3	1.6E+06 ( $\pm 10\%$ )
C-14	1.4E+04 ( $\pm 10\%$ )
Fe-55	2.4E+02 ( $\pm 10\%$ )
Co-60	2.9E+02 ( $\pm 13\%$ )
Sr-90	3.5E+04 ( $\pm 10\%$ )
Cs-134	6.5E+00 ( $\pm 22\%$ )
Cs-137	1.3E+04 ( $\pm 16\%$ )
Ba-133	9.3E+00 ( $\pm 24\%$ )
Eu-152	1.5E+02 ( $\pm 15\%$ )
Eu-154	1.7E+02 ( $\pm 6\%$ )
Eu-155	2.1E+01 ( $\pm 16\%$ )

\* Date of reference: 01/02/2010

**Table 4.1.4:** Radionuclide inventory of a typical sample from the reflector of the AVR reactor

Nuclide	Activity [Bq/g]
H-3	9.0E+06 ( $\pm 10\%$ )
C-14	3.3E+05 ( $\pm 10\%$ )
Fe-55	3.8E+03 ( $\pm 10\%$ )
Co-60	8.6E+03 ( $\pm 14\%$ )
Sr-90	2.4E+05 ( $\pm 10\%$ )
Cs-134	5.8E+01 ( $\pm 19\%$ )
Cs-137	2.2E+04 ( $\pm 16\%$ )
Ba-133	5.8E+02 ( $\pm 17\%$ )
Eu-152	n. d.
Eu-154	1.9E+02 ( $\pm 15\%$ )
Eu-155	6.5E+01 ( $\pm 23\%$ )

\* Date of reference: 01/02/2010



## 4.2 Samples investigated at CEA

### 4.2.1 G2 results

#### 4.2.1.1 Activity of the G2-36 core sample

The activities on each sample are summarised in Table 4.2.1 and Figure 4.2.1.

**Table 4.2.1:** Total activity of samples before leaching (date: 9 march 2004; the results are given with an uncertainty of  $\pm 10\%$  for samples No. 3, 7 and 11, and  $\pm 20\%$  for the others; one measurement per sample)

Sample activity [Bq/g]	$^{63}\text{Ni}$	$^{36}\text{Cl}$	$^{60}\text{Co}$	$^{14}\text{C}$	$^3\text{H}$	$^{137}\text{Cs}$	$^{133}\text{Ba}$	$^{154}\text{Eu}$	$^{155}\text{Eu}$
No. 2	3,060	216	453	8,600	36,000	37	25	93	14
No. 3	6,560	214	960	25,000	31,000	41	27	95	16
No. 5	6,544	283	1,420	13,000	44,000	66	28	110	21
No. 6	4,880	254	1,450	20,000	38,000	63	26	90	17
No. 7	8,110	183	1,800	25,000	46,000	71	29	100	18
No. 8	6,240	353	1,520	18,000	48,000	73	26	110	19
No. 9	6450	394	1,720	25,000	49,200	76	25	110	18
No. 10	5,340	510	1,510	31,000	55,000	85	26	120	17
No. 11	9,750	307	2,300	18,000	68,000	110	23	110	21

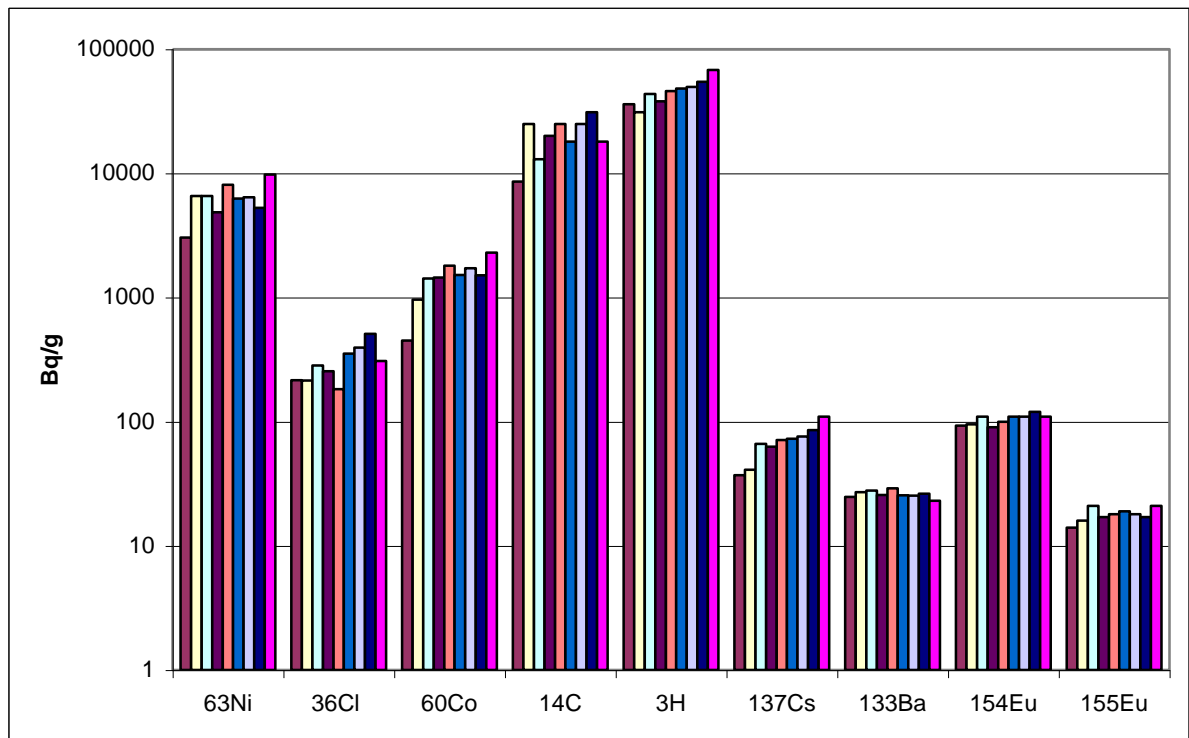


**Figure 4.2.1:** PROFILE of activity in the core sample (a relatively homogeneous distribution can be noted amongst the measurements uncertainties in most of the radioisotopes in the core sample, apart from in the <sup>137</sup>Cs, whose activity increases regularly between sample No. 2 and sample No. 11)

#### 4.2.1.2 Activity of core samples G2-27, G2-32, G2-42, G2-46

The results are shown in the Table 4.2.2. The results were provided on 14/11/09. One measurement was made per sample apart from <sup>36</sup>Cl. The results gave an uncertainty multiplied by a factor of  $k = 2$ .

**Table 4.2.2:** Radiochemical characterisations of SAMPLES from G2 (average powders case)

Isotope	G2-27 [Bq/g]	G2-32 [Bq/g]	G2-42 [Bq/g]	G2-46 [Bq/g]
$^3\text{H}$	$(3.5 \pm 0.2) \cdot 10^4$	$(4.2 \pm 0.4) \cdot 10^4$	$(4.2 \pm 0.3) \cdot 10^4$	$(1.4 \pm 0.1) \cdot 10^4$
$^{14}\text{C}$	$(2.57 \pm 0.16) \cdot 10^4$	$(2.24 \pm 0.15) \cdot 10^4$	$(1.23 \pm 0.08) \cdot 10^4$	$(4.6 \pm 0.3) \cdot 10^3$
$^{36}\text{Cl}$	$180 \pm 24$	$149 \pm 22$	$225 \pm 50$	$108 \pm 19$
$^{51}\text{Cr}$	$< 25$	$< 18$	$< 11$	$< 8$
$^{54}\text{Mn}$	$< 5$	$< 4$	$< 2$	$< 1.2$
$^{60}\text{Co}$	$880 \pm 50$	$1200 \pm 70$	$480 \pm 28$	$130 \pm 8$
$^{133}\text{Ba}$	$30 \pm 4$	$25 \pm 3$	$45 \pm 3$	$27 \pm 2$
$^{134}\text{Cs}$	$< 3$	$< 2.7$	$< 1.5$	$< 1.0$
$^{137}\text{Cs}$	$87 \pm 8$	$124 \pm 9$	$24 \pm 3$	$10 \pm 2$
$^{152}\text{Eu}$	$< 9$	$< 6$	$< 4$	$< 3$
$^{154}\text{Eu}$	$94 \pm 8$	$59 \pm 5$	$49 \pm 4$	$136 \pm 8$
$^{155}\text{Eu}$	$18 \pm 4$	$11 \pm 2$	$6 \pm 1$	$17 \pm 3$

It can be seen that, overall, the reflector is less active than the moderator. In the detail, the activity in  $^{14}\text{C}$  of the graphite decreases in accordance with the position in the stack, while the activity of  $^3\text{H}$  appears to be more or less constant on the samples from the moderator. The measurements by gamma spectrometry also indicate the presence of  $^{137}\text{Cs}$ , tracer of fission products, with an activity of round about one hundred Bq/g in samples 27-32, and then weaker activity in the other two. It can be seen that activities of  $^{36}\text{Cl}$  are rounded one hundred Bq/g, which is quite consistent with the values obtained on the G2-36 core sample.

#### 4.2.2 Samples removed from core samples

Measurements of  $^{36}\text{Cl}$  have also been made on the small samples from each end, and in the middle of the core samples (see Table 4.2.3 and Figure 4.2.2).

**Table 4.2.3:** Measurement of  $^{36}\text{Cl}$  samples from G2 core samples (2 tests made; results provided with uncertainty extending to  $k = 2$  on 01/12/08)

Sample Pos.	$^{36}\text{Cl}$ [Bq/g]	Sample Pos.	$^{36}\text{Cl}$ [Bq/g]
G2-27 End 1	$230 \pm 27$	G2-32 End 1	$190 \pm 25$
G2-27 Middle	$180 \pm 24$	G2-32 Middle	$123 \pm 14$
G2-27 End 2	$256 \pm 30$	G2-32 End 2	$211 \pm 24$
G2-42 End 1	$698 \pm 80$	G2-46 End 1	$7 \pm 1$

G2-42 Middle	135±17	G2-46 Middle	115±17
G2-42 End 2	1316±150	G2-46 End 2	15±2

These values reveal more or less marked heterogeneity in the activities in  $^{36}\text{Cl}$  in the samples. The graphs below show the values according to the position of the samples compared to the average value obtained on the powders from specimens.

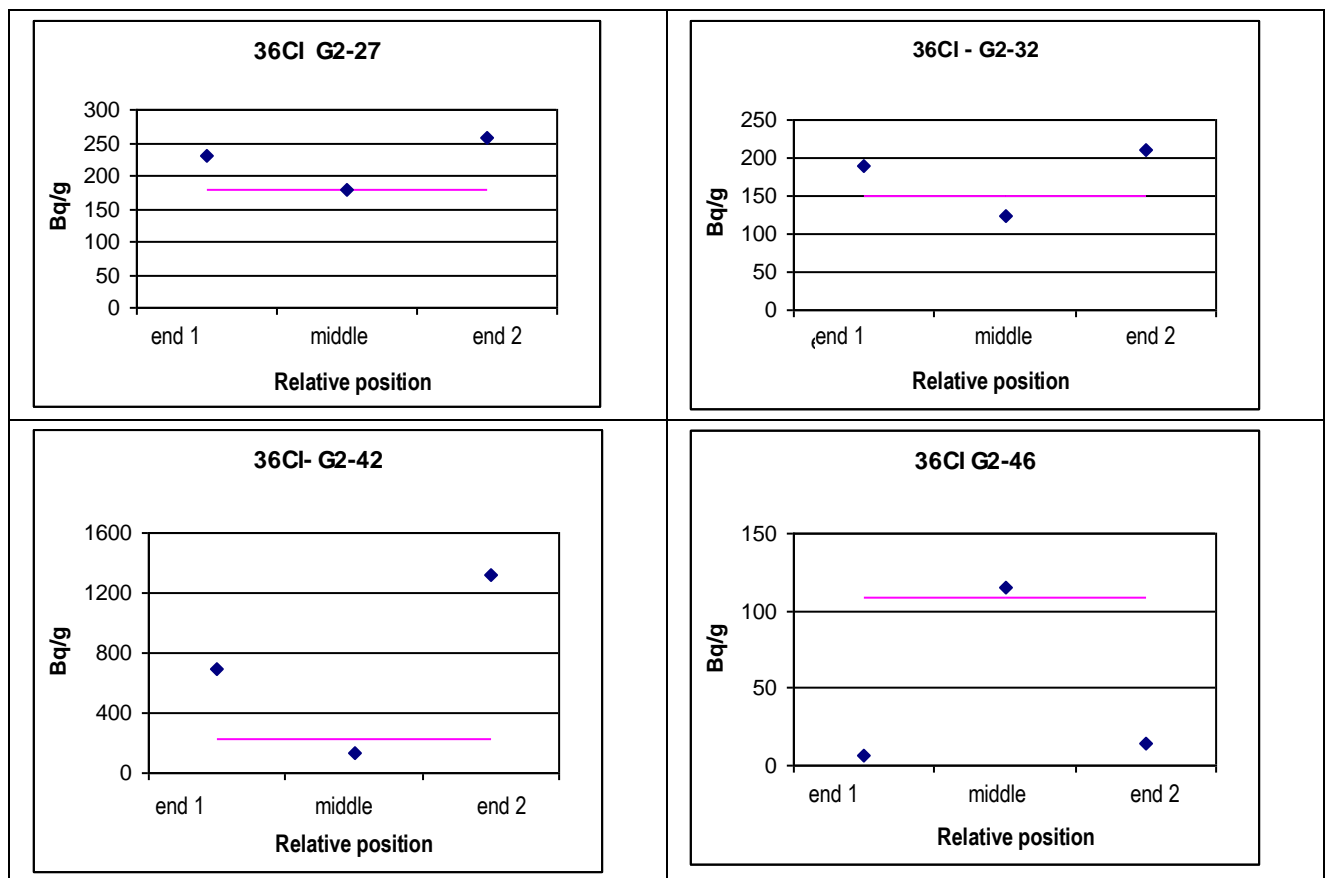


**Figure 4.2.2:** Distribution of CHLORINE 36 in samples

#### 4.2.3 St Laurent A2 results

To date, the only results available are from measurements by gamma spectrometry on the entire solid samples (see Table 4.2.4).

**Table 4.2.4:** Activity of gamma emitters calculated by gamma spectrometry on the entire solid samples

Ref.	<sup>60</sup> Co [Bq/g]	<sup>133</sup> Ba [Bq/g]	<sup>134</sup> Cs [Bq/g]	<sup>137</sup> Cs [Bq/g]	<sup>154</sup> Eu [Bq/g]	<sup>155</sup> Eu [Bq/g]
SLA2-103	2.3E+04	2.6E+01	1.2E+01	2.4E+01	5.0E+01	9.2E+00
SLA2-105	1.5E+04	1.4E+02	2.9E+01	4.6E+01	1.4E+02	< LD
SLA2-110	4.7E+04	8.0E+01	1.3E+01	1.0E+02	7.8E+01	1.7E+01
SLA2-116	9.1E+03	7.4E+00	1.3E+01	9.0E+00	1.9E+01	7.0E+00
SLA2-119	3.6E+02	9.5E+00	9.1E+00	3.1E+00	1.0E+02	2.0E+01
SLA2-63	2.15E+04	2.86E+01	1.85E+01	< LD	3.66E+01	1.35E+01
SLA2-65	7.47E+03	1.12E+02	2.99E+01	1.76E+01	7.47E+01	2.19E+01
SLA2-71	1.04E+04	2.33E+01	< LD	2.20E+01	1.68E+01	7.34E+00
SLA2-76	1.18E+04	0.00E+00	6.76E+00	1.27E+01	8.88E+01	2.20E+01
SLA2-79	4.09E+03	1.50E+01	< LD	8.19E+00	2.27E+02	4.14E+01

### 4.3 Samples investigated at CIEMAT

*/CIEMAT/ results on characterization of sample material*

### 4.4 Samples investigated at ENEA

The characterisation activities were firstly postponed waiting for the pending arrival of the requested samples from Romanian Reactor. Due to the unavailability of those samples, the activities were recently shifted on the Latina NPP graphite. Unfortunately, due to a contamination event arisen in the laboratory during another experiment, the area is actually not accessible, so that the data (dimensions, weight and inventory) for each sample are not available and the gamma measurements have been stopped till the complete radiological restoration of the area (foreseen for the middle of May).

For this reason only one sample's data are available and has been already characterized: it is the one labelled 04F04A1/I1, a prismatic one, taken from the inferior surface of a graphite brick, in the central channel (A1) at the bottom of the active core. The dimensions are 1.5 x 1.0 x 0.5 cm, and the weight is 1.8 grams.

**Table 4.4.1:** Main gamma emitters inventory for i-graphite from Latina NPP

Nuclide	Sample 04F04A1/I1	
	Activity [Bq/g]	Uncert. [%]
<sup>60</sup> Co	1604.9	0.4
<sup>137</sup> Cs	25.3	9.6
<sup>133</sup> Ba	51.7	4.2
<sup>154</sup> Eu	53.1	11.1
<sup>155</sup> Eu	12.5	17.1

#### 4.5 Samples investigated at FI

The results of gamma spectrometry analysis of the sub-samples GR-211, GR-212 and GR-213, which represent the inner surface of the bulk graphite sample GR16, as well as the results for the sub-samples GR-221, GR-222 and GR-223, which represent the outer surface of the sample GR16 are summarized in Table 4.5.1.

**Table 4.5.1:** Gamma-ray emitters in graphite sleeve of RBMK-1500 reactor

Sample code	Activity concentration of radionuclides, Bq/g (1σ)						
	Mn-54	Co-60	Cs-134	Cs-137	Eu-152	Eu-154	Eu-155
GR-211	1.5±0.2	350±50	<0.10	2.2±0.2	15.5±3.1	3.3±0.7	0.46±0.09
GR-212	0.46±0.07	68±10	0.44±0.11	2.7±0.3	13.1±2.6	3.2±0.6	0.53±0.11
GR-213	0.37±0.06	35±6	0.43±0.11	2.2±0.2	13.5±2.7	2.7±0.5	0.33±0.07
Mean	0.8	152	0.29	2.4	14.0	3.1	0.44
StDev	0.6	175	0.25	0.3	1.2	0.3	0.10
GR-221	0.18±0.03	38±6	0.39±0.10	3.4±0.3	11.8±2.4	3.0±0.6	0.56±0.11
GR-222	0.11±0.02	26±4	0.18±0.05	4.1±0.4	11.7±2.3	3.2±0.6	0.67±0.13
GR-223	0.10±0.02	40±6	0.18±0.05	2.8±0.3	11.9±2.4	2.6±0.5	0.46±0.09
Mean	0.13	35	0.25	3.4	11.8	2.9	0.57
StDev	0.04	8	0.12	0.6	0.1	0.3	0.11

Results show that inhomogeneity is noticeable for corrosion products Mn-54 and Co-60. Distribution of activity of fission products Cs-137 and Eu isotopes is rather homogeneous.

The main part of activity in the irradiated graphite samples originates from radiocarbon. Its activity concentration is at least higher by 2–3 orders of magnitude than that of the corrosion product Co-60. The measured values of C-14 activity are considerably higher than calculated values of C-14 activity in the graphite constructions of the RBMK-1500 reactor as it is presented in Table 4.5.2.



**Table 4.5.2:** Activity of radionuclide C-14 in the RBMK-1500 graphite constructions

A (14C), kBq/g	Stack	Graphite construction		
		Sleeve (Gr.13, Gr.14)	Top reflector (Gr.18)	Bottom reflector (Gr.16)
Simulated values from C-13(n, $\gamma$ )C-14 reaction	42.7	35.2	7.4	7.4
Experimental values		130 $\pm$ 20	13 $\pm$ 4	24 $\pm$ 6

This can be explained by the fact that C-14 is also produced in N-14(n,p)C-14 reaction, which was not taken into account by MCNPX calculations. Nitrogen is used to flush the graphite stack of the RBMK-1500 reactors. Therefore, one can expect that its activation reaction mostly occurs on the surface (30 nm according to Ref. 4.5.1) of graphite where non-negligible amount of N-14 from cooling gas of the core cooling gas circuit can be accumulated. The impurities of N-14 in the graphite stack comprise 0.5–70 ppm as reported in Ref. 4.5.1. Taken into account this concentration the amount of C-14 produced in N-14(n,p)C-14 reaction has been calculated by MCNPX. The lowest N-14 concentration range corresponds to an increase of C-14 activity by 18%, and the highest concentration range corresponds to an increase of C-14 activity by 25 times. As one can see the experimental value of C-14 activity is 3.7 times higher than the simulated value (see Table 4.5.2).

Taking into account experimentally determined C-14 specific activity (130 $\pm$ 20 kBq/g) and published data on N-14 [4.5.2], one can conclude that N-14 concentration in graphite is 7.6 $\pm$ 2.0 ppm.

Activity of radiochlorine (Cl-36) of the bottom reflector of the RBMK-1500 reactor has been found to be below detection limit of the liquid scintillation counting techniques.

## 4.6 Samples investigated at INR

The results obtained on the i-graphite samples from the thermal column of TRIGA reactor are presented in this chapter. Figure 4.6.1 shows the locations selected for i-graphite sampling in view of characterization.

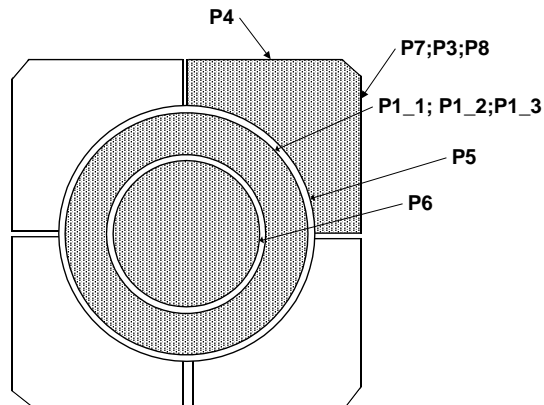


**Figure 4.6.1:** Locations selected for i-graphite sampling in view of characterization

The sample prepared from central cylindrical piece of the cell (sample P6) was divided in different aliquots, so that 6 aliquots for determination of  $\beta/\gamma$ -emitting radionuclides and 3 aliquots for C-14 content determination have been made and measured. The identified  $\beta/\gamma$ -emitting radionuclides were: Co-60, Cs-137, Eu-152 and Eu-154. The results of the  $\beta/\gamma$ -emitting radionuclides and C-14 activity are presented in Figure 4.6.2.

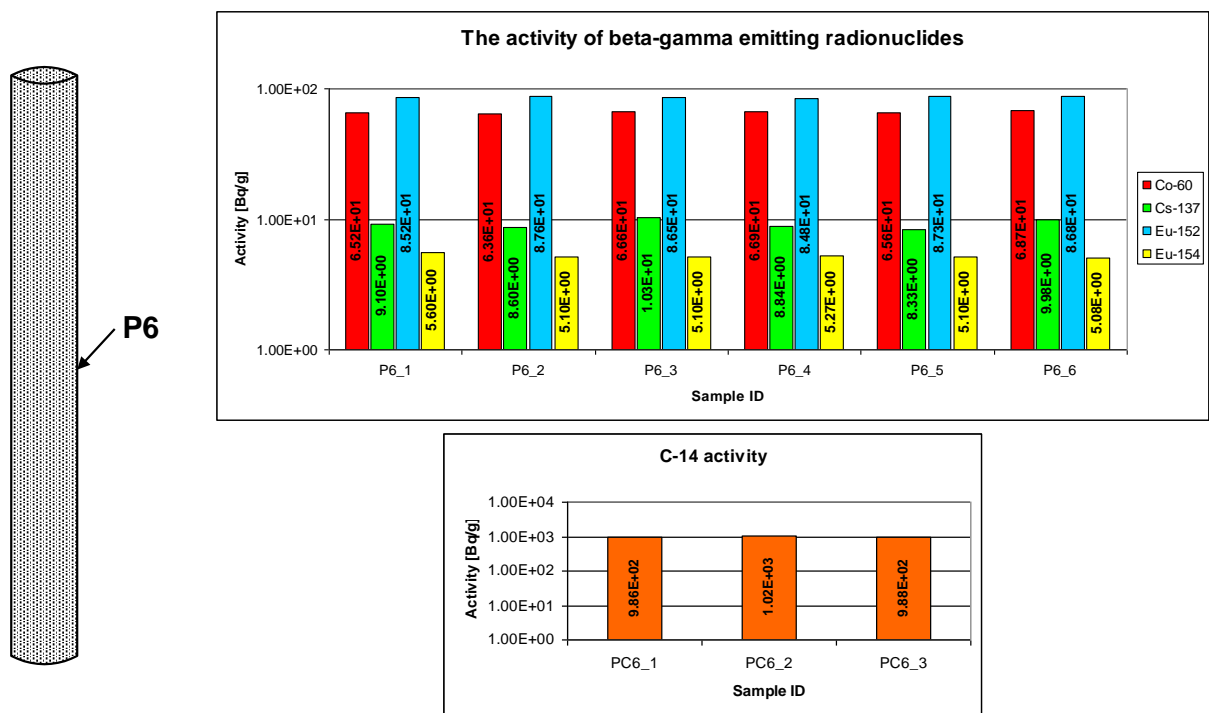


**Figure 4.6.2:** The samples' activity from central cylindrical piece of the cell (P6)

There are two different hypothesis related to the provenance of Co-60 and Eu-152 in i-graphite:

- The first, activation of initial impurities existing in the virgin graphite;

- The second, contamination arising from the melting points of aluminium cladding.

The activity of Cs-137 is very low, close of minimum detectable activity. Besides the C-14 activity from i-graphite this is about 1 kBq/g and arises mainly from nitrogen activation.

The activities of  $\beta/\gamma$ -emitting radionuclides for the 6 aliquots prepared from the sample situated on the external surface of the upper part on the pipe piece (sample P1\_1) are presented in Figure 4.6.3. The measured activities are higher than the activities determined for the sample from central cylindrical piece.

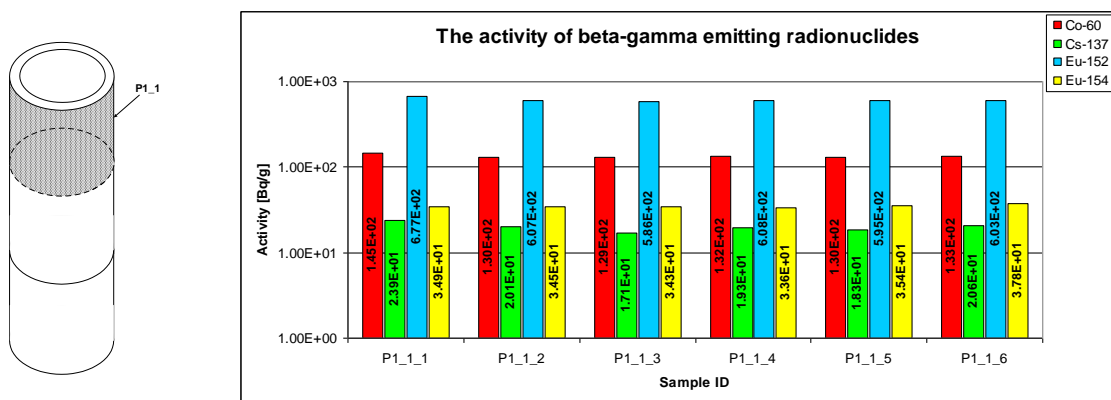


**Figure 4.6.3:** The samples' activity situated on the external surface of the upper part on the pipe piece (P1\_1)

The activity of  $\beta/\gamma$ -emitting radionuclides for the 5 aliquots prepared from the sample situated on the external surface of the middle part on the pipe piece (sample P1\_2) and the C-14 activity for the 3 aliquots prepared from the same sample are presented in Figure 4.6.4. Only for this part of the piece we determined all kinds of measurements: determination of  $\beta/\gamma$ -emitting radionuclides and C-14 activity. We observed that the C-14 activity for the sample from this piece is very little higher than the activity for the sample from the central cylindrical piece.

The reason to determine the C-14 activity only for this part of pipe piece is because in this stage of our measurements we wanted to determine the variation of the activity from the inside to the outside only for the middle part of the cell.

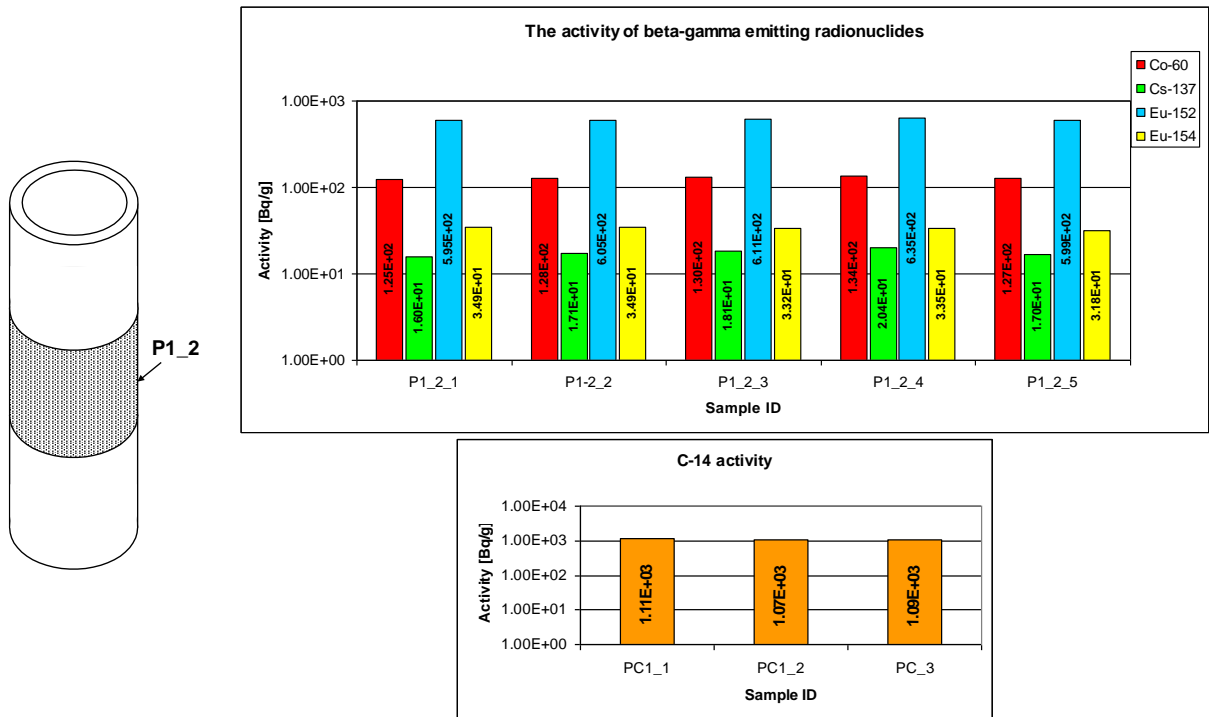


**Figure 4.6.4:** The samples' activity situated on the external surface of the middle part on the pipe piece (P1\_2)

In Figure 4.6.5 are presented the activities of  $\beta/\gamma$ -emitting radionuclides for the aliquots prepared from the sample located at the bottom part of the pipe piece (sample P1\_3).

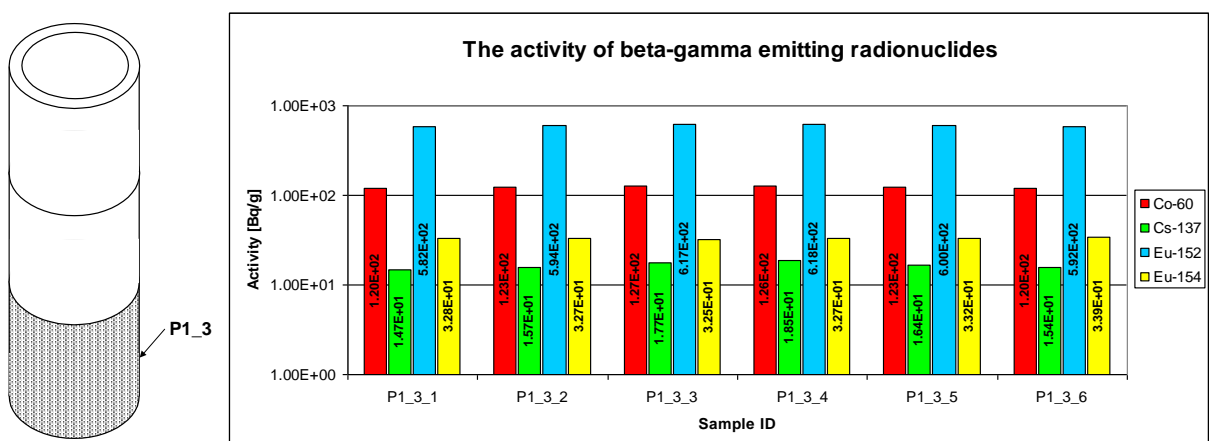


**Figure 4.6.5:** The samples' activity situated on the external surface of the bottom part on the pipe piece (P1\_3)

The results for the sample prepared from the cylindrical internal surface of the piece located in one of the cell corners (sample P5) are presented in Figure 4.6.6 The sample was prepared from the middle part of this piece, so we performed all types of measurements.

An interesting result is that for this piece the C-14 activity is lower than the C-14 activity for the previous internal piece. Also the Co-60 activity is very little lower than the Co-60 activity for previous pieces while the activity of the various europium radionuclides rise up.

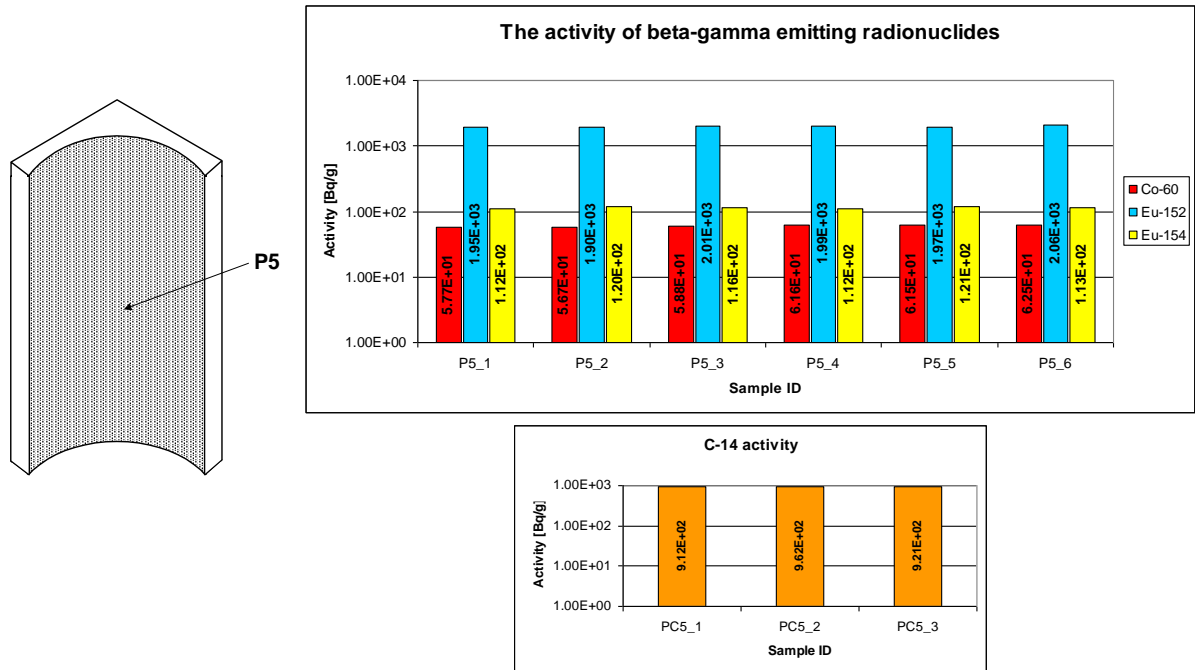


**Figure 4.6.6:** The samples' activity situated on the cylindrical internal surface of the middle part of the piece located in one of the cell corners (P5)

In Figures 4.6.7–10 are presented the results for the samples prepared from external surface of i-graphite cell. For all of the four locations the activity of Cs-137 was below detection limit, and for the samples prepared from the middle part of piece located in the cell corner (samples P3 and P4) all two kinds of measurements have been performed. The  $\gamma$ -ray spectrometry analyses indicate a very little difference between activities from two contiguous faces (see Figures 4.6.9 and 10).

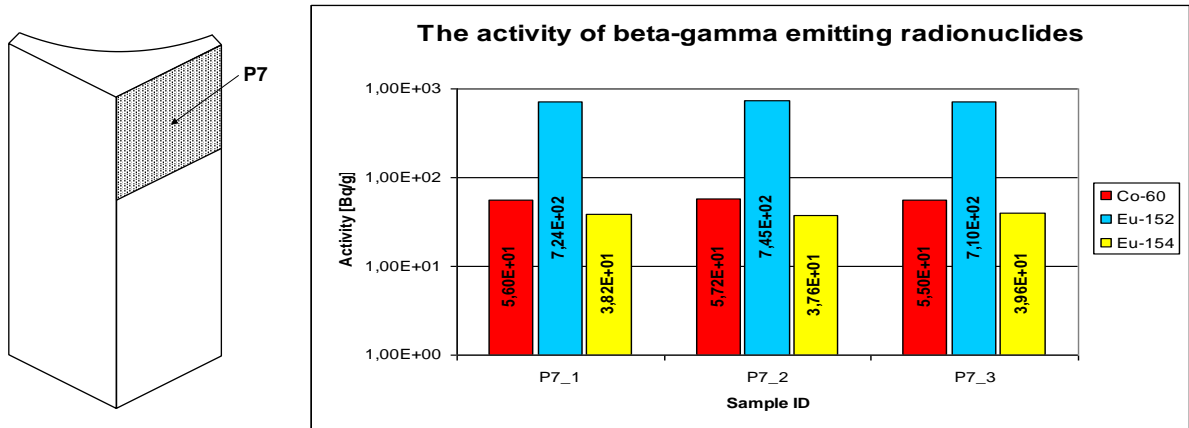


**Figure 4.6.7:** The samples' activity situated on the external surface of the upper part of the piece located in the cell corners (P7)

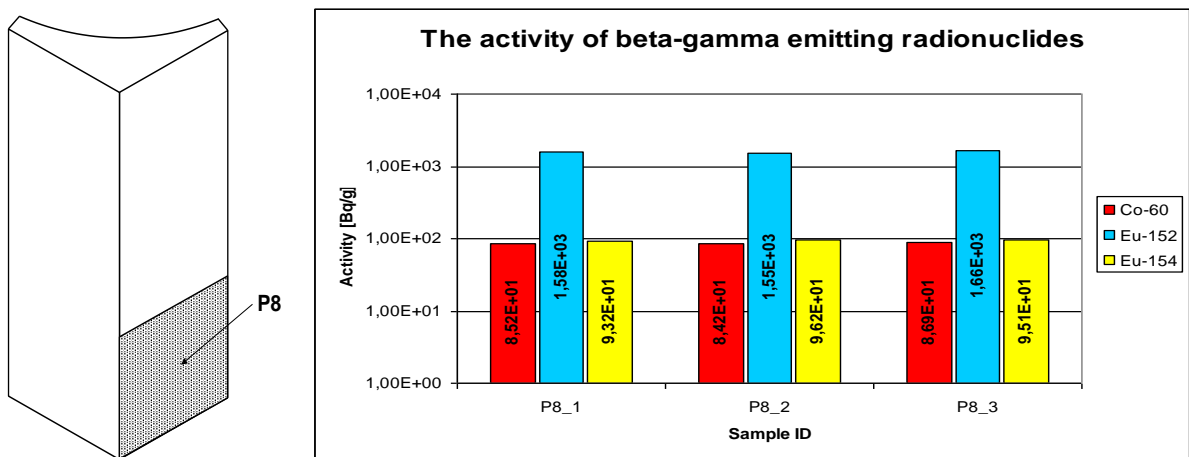


**Figure 4.6.8:** The samples' activity situated on the external surface of the bottom part of the piece located in the cell corners (P8)



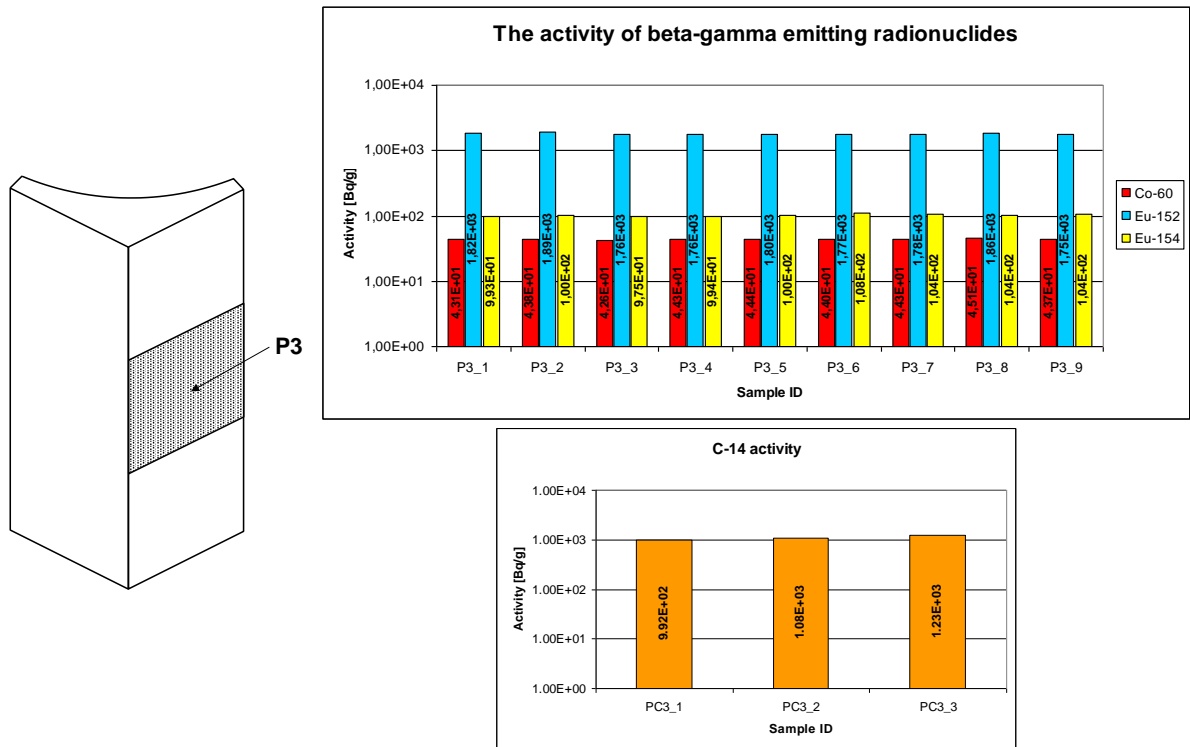


**Figure 4.6.9:** The samples' activity situated on the external surface of the middle part on the piece located in one of the cell corners (P3)

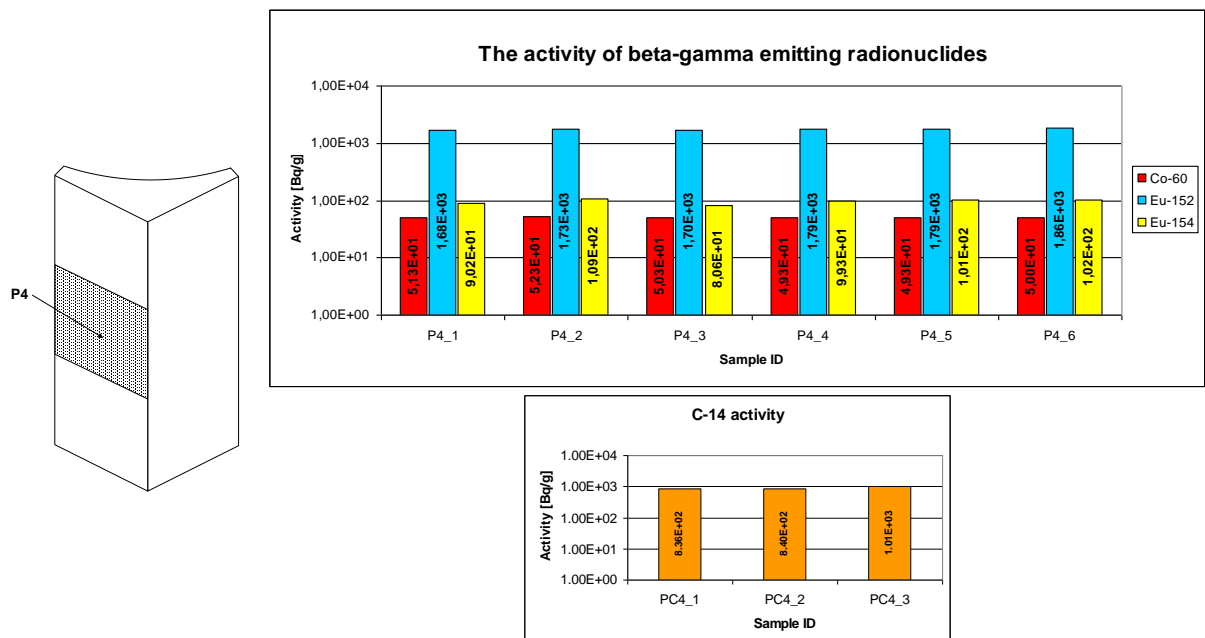


**Figure 4.6.10:** The samples' activity situated on the external surface of the middle part on the piece located in one of the cell corners (another face) (P4)

From the measurements performed on the samples from external surface of the piece located in the cell corner one can approximate that the activity for the main identified  $\beta/\gamma$ -emitting radionuclides increase from the top to the bottom of the piece. In the case of C-14 activity it is clear that it increase from the top to the bottom of the piece. The results achieved until now show Figure 4.6.11:

- The activity of europium radionuclides decrease from the outside to the inside of the cell;
- The activity of Co-60 has an unclear variation;
- C-14 activity increase from the top to the bottom of the cell, but only for the piece from the corner.

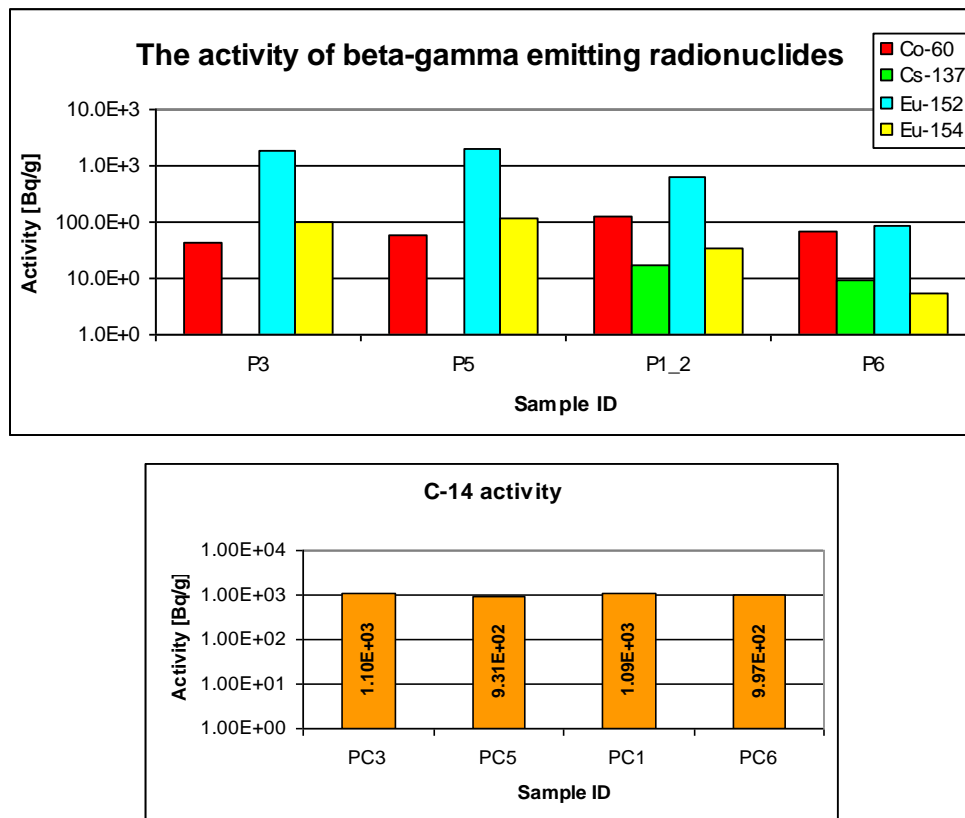


**Figure 4.6.11:** Variation of activity in the cell (from the outside to the inside)

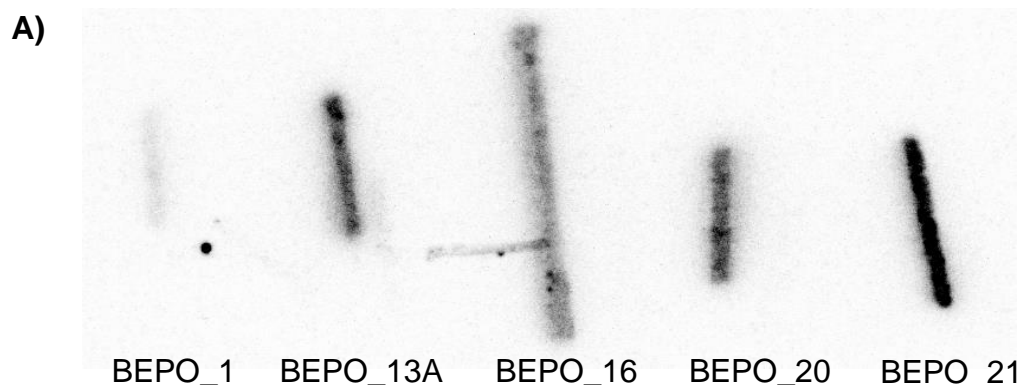
#### 4.7 Samples investigated at SCK.CEN

Results are not yet available since the MTR samples were not yet distributed.

## 4.8 Samples investigated at UoM

Inspection of a typical reconstructed CT volume of graphite shows clearly identifiable pores within the graphite matrix. These can be segmented and examined quantitatively in three dimensions. In some samples areas of high attenuation were observed. These high attenuation areas could be broadly divided into 2 types: spots and smears. Spots were highly localised areas with a greyscale value (attenuation) that saturated at the maximum, and smears were larger areas where the greyscale value was noticeably higher than the average of the surrounding material. Attenuation is proportional to the density of the material of constant atomic number, and the attenuation in these areas is too high for them to be due variations in graphite density. It was important to determine the composition of the high attenuation areas to determine their origin. In the reactor certain elements can be transmuted into radioactive isotopes, and their location and ease of transport within the porous microstructure have implications for graphite decommissioning.

Autoradiography was carried out on all BEPO samples in order to gain a qualitative assessment of the distribution of radioisotopes within the irradiated BEPO material. Figure 4.8.1 shows the average intensity of the samples with increasing sample number  $s$  after an exposure time of 20 hours. Sample 1 exhibits the least intensity of the BEPO materials, which corresponds to the least active samples  $s$ . There is a non uniform distribution of radioisotopes which can be noted by the presence of high intensity regions contained within sample 16. This is also a high distribution of activity with both sample 20 and 21. This film is fully saturated and again shows a non uniform disruption of  $\beta$  and  $\gamma$  activity within the sample.



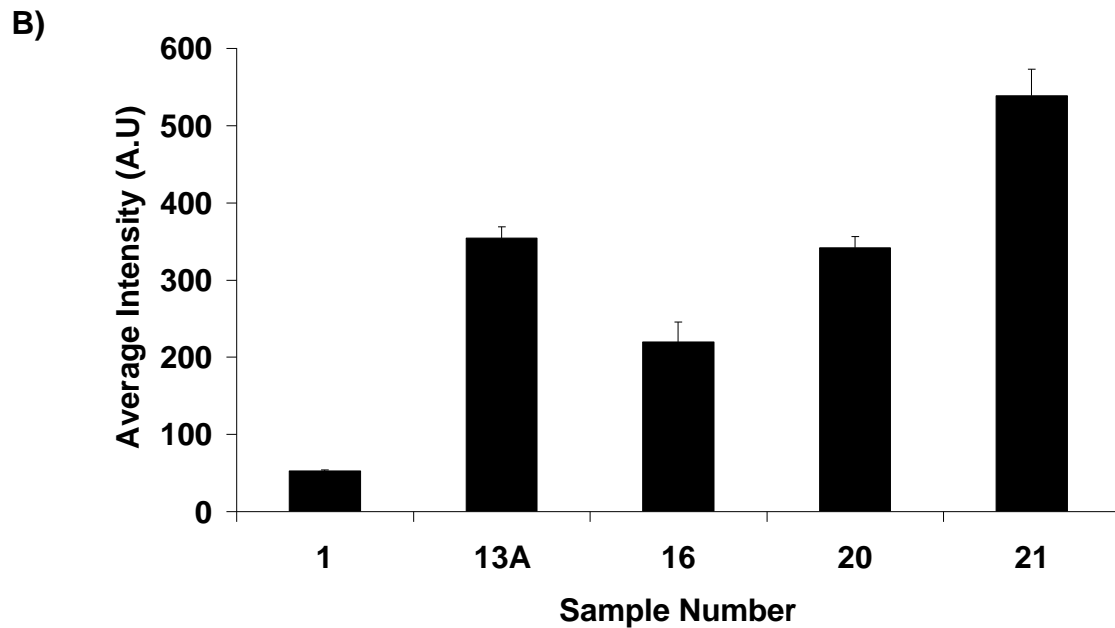


**Figure 4.8.1:** A) Autoradiograph showing increasing greyscale intensities with exposed BEPO samples, B) graph showing the average intensity for BEPO samples

#### 4.9 Samples investigated at ENS / IPNL?

## 5. Compilation of Results

*/CIEMAT, FZJ/ Compilation of results in an Excel Sheet compatible to Database Needs*

## 6. Evaluation for Direct Disposal

*/EMN, ANDRA, ENRESA, NDA/ Compilation of criteria for direct disposal*

## 7. Summary

*/FZJ/ Publishable summary*

## 8. References

*Compilation of related literature* (Format: [Chapter N°.x] (e.g. [2.3], i.e. third reference in Chapter 2)

- [3.1.1] Bisplinghoff, B.; Lochny, M.; Fachinger, J.; Brücher, H. 1999. Radiochemical Characterisation of Graphite from Jülich Experimental Reactor (AVR). In *Proceedings of the Technical Committee Meeting: Nuclear Graphite Waste Management*. Manchester, United Kingdom, 18–20 October 1999: International Atomic Energy Agency.
- [4.5.1] Ancius, D.; Ridikas, D.; Remeikis, V.; Plukis, A.; Plukiene, R.; Cometto, M. 2005. Evaluation of the activity of irradiated graphite in the Ignalina Nuclear Power Plant RBMK-1500 reactor. *Nukleonika* 50(3): 113–120.
- [4.5.2] Takahashi, R.; Toyahara, M.; Maruki, S.; Ueda, H. 1999. Investigation of morphology and impurity of nuclear grade graphite and leaching mechanism of Carbon-14. In *Proceedings of the Technical Committee Meeting: Nuclear Graphite Waste Management*. Manchester, United Kingdom, 18–20 October 1999: International Atomic Energy Agency.